Review article

Evolution of arc magmatic cycles from the Carboniferous to the Early Cretaceous in the western paleomargin of Gondwana, north of the Andes

Evolución de los ciclos magmáticos de arco desde el Carbonífero hasta el Cretácico Temprano, en la paleomargen occidental de Gondwana, norte de los Andes

Gabriel **Rodríguez García**[1], Ana María **Correa Martínez**[1], Juan Pablo **Zapata**[1], Diego Armando **Ramírez**[1], Carlos Andrés **Sabrica**[1]

1. Servicio Geológico Colombiano, Special Geological Studies Group, Medellín, Colombia.
Corresponding author: Gabriel Rodríguez García, grodríguez@sgc.gov.co

Abstract

This work presents a considerable volume of new and compiled data indicating that arc magmatism in the western paleomargin of Gondwana began in the Carboniferous and continued during the Permian and Early Triassic. Subsequently, the magmatism reactivated during the Early and Middle Jurassic due to the subduction of the Farallon Plate under the continental paleomargin. The arc pluton belts are distributed from the edge of the paleomargin toward the interior of the continent in the same orientation as the slab (west–east direction).

During the Carboniferous, between ca. 333 Ma and ca. 300 Ma, magmatism formed small calcic metaluminous gabbro and leucotonalite plutons of tholeiitic to calc-alkaline affinity on the western margin of Gondwana. Later, the second belt of arc plutons formed during the Permian/Triassic (between ca. 300 Ma and ca. 234 Ma) and are represented by metaluminous to peraluminous calc-alkaline to high-K calc-alkaline batholiths and stocks of heterogeneous composition (granites, granodiorites, diorites, quartz monzonites, and monzonites), which were intruded by dikes and minor granite bodies during the Middle Triassic.

Between ca. 214 Ma and ca. 186 Ma, peraluminous plutons of batholithic dimensions of monzogranitic to syenogranitic composition developed in the back-arc. Between ca. 197 Ma and ca. 186 Ma, back-arc magmatism occurred, while a new magmatic cycle began along the arc axis. At the end of the Jurassic, the magmatic arc cycle ended in the northwestern paleomargin of Gondwana (ca. 164 Ma). The intrusion ca. 159 Ma of porphyritic bodies of alkaline andesitic basalts toward the edge of the continental margin suggests the strangulation and collapse of the subduction zone in the mantle.

To the west, off the continental margin, a new arc magmatic cycle began over a different continental terrane ca. 171 Ma and extended to ca. 138 Ma, giving rise to a belt of calcic to calcic-alkaline plutons emplaced in the Ordovician metamorphic (Anacona Terrane), Triassic (Tahamí Terrane), and Upper Jurassic (Tierradentro Orogen) rocks. The assemblage amalgamated to the western margin of Gondwana in this period.

Keywords: Colombia, arc magmatism, evolution of the Andes.

Resumen

Este trabajo presenta un volumen considerable de datos, nuevos y compilados, los cuales indican que el magmatismo de arco, en la paleomargen occidental de Gondwana, inició en el Carbonífero, continuó en el Pérmico y tuvo un evento menor a principios del Triásico. Posteriormente el magmatismo se reactivó durante el Jurásico Temprano y Medio debido a la subducción de la placa Farallones bajo la paleomargen continental de Gondwana. Los cinturones de plutones de arco se distribuyen desde el borde de la paleomargen hacia el interior del continente, en el mismo sentido del slab, es decir, en dirección oeste-este.

Durante el Carbonífero, entre ca. 333 Ma y ca. 300 Ma, inició un magmatismo que formó pequeños plutones de gabros y leucotonalitas toleíticos a calco-alcalinos, metaluminosos cálcicos, el cual se localizó en la margen occidental de Gondwana. Inmediatamente después se formó un segundo cinturón de plutones de arco durante el Pérmico (entre ca. 300 Ma y ca. 234 Ma), representado por batolitos y stocks de composición heterogénea (granitos, granodioritas, dioritas, cuarzomonzonitas y monzonitas), calco-alcalinos a calco-alcalinos de alto K, metaluminosos a peraluminosos, de granitoides cálcicos, calco-alcalinos y alcalino-cálcicos, los cuales fueron intruidos por diques y cuerpos menores de granitos durante el Triásico Medio.

Entre ca. 214 Ma y ca. 186 Ma se presentó magmatismo peraluminoso de composición monzogranítica a sienogranítica en el trasarco, y se formaron plutones de dimensiones batolíticas. Entre ca. 197 Ma y ca. 186 Ma, el magmatismo de trasarco ocurrió al tiempo que inició un nuevo ciclo magmático en el eje del arco. A finales del Jurásico finalizó el ciclo magmático de arco en la paleomargen noroccidental de Gondwana (ca. 164 Ma). La intrusión a ca.159 Ma de cuerpos porfídicos de basaltos andesíticos alcalinos, hacia el borde de la margen continental, sugiere el estrangulamiento y el colapso de la zona de subducción en el manto.

Al occidente, por fuera de la margen continental, comenzó un nuevo ciclo magmático de arco sobre otra masa continental a ca. 171 Ma y se extendió hasta ca. 138 Ma, dando origen a un cinturón de plutones cálcicos a cálcico-alcalinos emplazado en rocas metamórficas del Ordovícico (terreno Anacona), Triásico (terreno Tahamí) y Jurásico Superior (Orogéno de Tierradentro). El conjunto fue amalgamado a la margen occidental de Gondwana en este periodo.

Palabras clave: Colombia, magmatismo de arco, evolución de los Andes.

1. Introduction

Among the problems of the Carboniferous to Cretaceous magmatic interpretations of the northwestern paleomargin of South America are, until a few years ago, the lack of available U–Pb geochronology and whole-rock geochemistry data, the regional separation and grouping of the plutonic and volcanic bodies, and their spatial correlation. This uncertainty has resulted in the use of geological units that belong to different magmatic events in the interpretations.

Arc magmatism in the western paleomargin of Gondwana has been considered to have begun at the end of the Triassic and continued until the Lower Cretaceous due to the subduction of the Farallon Plate under the western margin of Gondwana (Álvarez, 1983; Bayona et al., 1994; Bustamante et al., 2016; Jaramillo and Escovar, 1980; Leal-Mejía, 2011; Leal-Mejía et al., 2019; Rodríguez et al., 2015f, 2018, 2020; Quandt et al., 2018; Quiceno et al., 2016; Spikings et al., 2015; Toussaint, 1995; Villagómez et al., 2015; Zapata et al., 2016; Zuluaga et al., 2015; Zuluaga and López, 2019). Under this framework, two models were postulated: 1) migration of arc magmatism in an east–west direction (Bayona et al., 2010; Bustamante et al., 2016; Leal-Mejía et al., 2019; López and Zuluaga, 2020; Quandt et al., 2018; Ramírez et al., 2020; Zuluaga and López, 2019) and 2) migration of magmatism in a west–east direction (taking into account the migration of the magmatic cycles of the Permian and the Early to Middle Jurassic) (Rodríguez et al., 2018; 2020a, 2020b).
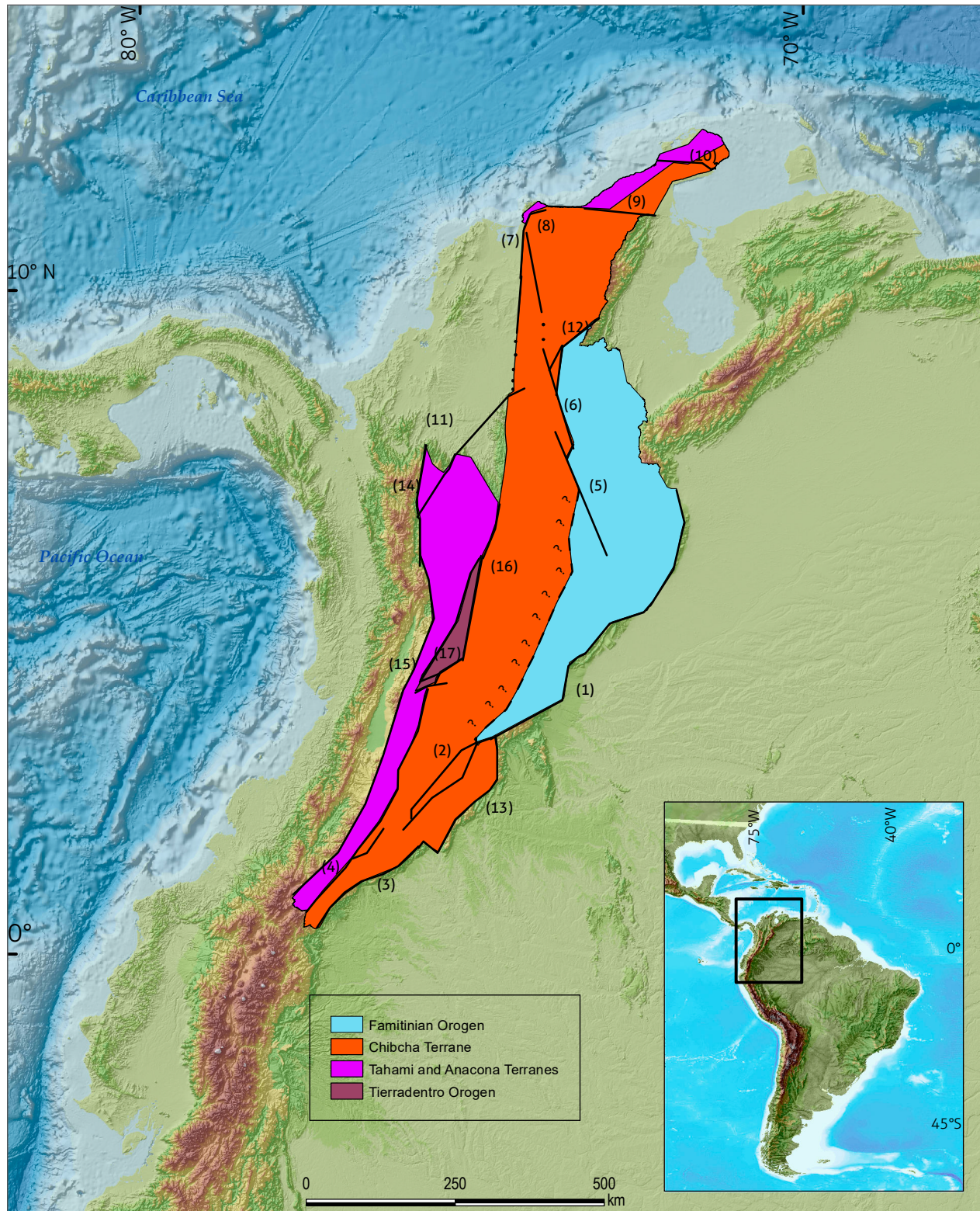
Figure 1. Terrains and orogens where the Carboniferous to Lower Cretaceous magmatic cycles were emplaced
1. Eastern Fault System; 2. Algeciras Fault System; 3. Los Loros Fault System; 4. San Francisco - Yungillo Fault System; 5. Bucaramanga Fault; 6. Ocaña Fault; 7. Santa Marta Fault; 8. Orihueca Fault; 9. Oca Fault; 10. Cuisa Fault; 11. Espíritu Santo Fault; 12. Arenas Blancas Fault; 13. Caguán System Fault; 14. Romeral Fault System; 15. San Jerónimo Fault; 16. Palestina Fault; 17. Ibagué Fault.

In this work, nine U–Pb zircon ages are reported, whose importance lies in the discovery of three new units that were not previously described in the literature on the geology of Colombia and the improvement in the information of the three other units. In addition, this paper presents a considerable volume of published ages derived from the research conducted by the Servicio Geológico Colombiano. The information on the whole-rock geochemistry of numerous plutons is also supplemented. This research analyzes the magmatic cycles formed from the Carboniferous to the Lower Cretaceous, the zircons inherited from the initial cycles, the geochemical composition of each cycle, and the geotectonic position of the magmatic belts with respect to the paleomargin of Gondwana in northern South America. In addition, a correlation is drawn of the units constituting the belts that make up a magmatic cycle and the position they currently occupy in the Andes of Colombia.

This study seeks to clarify the magmatic evolution of the arcs between the Carboniferous and the Lower Cretaceous, showing the correlation of units that make up each cycle, and presenting the development model of the magmatic cycles in the continental paleomargin of northwestern South America.

2. Geological framework

The western margin of Gondwana in northern South America was formed up to the Carboniferous by the Guyana Shield (northern half of the Amazonian Craton), which is currently located east of Colombia and is represented by units with ages of 2.5-1.5 Ga (Priem et al., 1982; Restrepo-Pace and Cediel, 2019). The western part of this shield in Colombia is composed of granitoids and high-grade metamorphic rocks that are part of the Río Negro Belt (1.84-1.72 Ga) (Kroonemberg, 2019; Tassinari 1981; Tassinari and Macambira, 1999), which is intruded by anorogenic granitoids of 1.55 Ga, such as the Parguaza Rapakivi Granite, and locally covered by sandstones and meta-sandstones of Naquén, Pradera, and Tunuí (Kroonemberg, 2019).

The Andean margin currently rises to the west of the cratonic domain, and it is composed of a basement of high-grade metamorphic rocks (granulite to high amphibolite facies) along with some igneous bodies probably formed during the continental collision of Amazonia and Laurentia during the Grenville Orogeny (Cordani et al., 2010; Ibáñez-Mejía et al., 2011; Kroonenberg 1982; Kroonemberg, 2019). The units that make up the Andean margin are the Garzón Group, Mancagua and Guapotón gneisses, Las Minas migmatites, El Recreo gra-

nite, San Lucas gneiss, Los Mangos granulite, Buritaca gneiss, and Jojoncito gneiss (Cuadros, 2012; Cuadros et al., 2014; Ibáñez-Mejía et al., 2011, 2015; Jiménez Mejía et al., 2006; Kroonenberg and Diederix, 1982; Ordoñez-Carmona et al., 2002; Piraquive, 2017; Rodríguez, 1995a, b; Rodríguez et al., 2003; Tschanz et al., 1969; Tschanz et al., 1974; Velandia et al., 1996, 2001). These units present ages between 1.2 and 0.85 Ga (Ibáñez et al., 2011, 2015) and are denominated in some studies as the Chibcha Terrane (Figure 1) (Restrepo and Toussaint, 1989, 2020; Restrepo et al., 2009) or the Putumayo Orogen (Ibáñez et al., 2011, 2015). On this basement, arc magmatic belts were developed during the Carboniferous, Permian, and Early to Middle Jurassic, extending from northern (the upper Guajira and Sierra Nevada) to southern Colombia and into Ecuador (Figure 2).

Lower Paleozoic (Figure 1) and Ordovician rocks (Mantilla et al., 2016; Restrepo-Pace, 1995) are found between the Amazonian Craton and the Chibcha Terrane (in the Santander, Floresta, Quetame, and Mérida Andes massifs), extending in fragments from Chile to Venezuela along the western protomargin of Gondwana (Otamendi et al., 2017; Ramos, 2008). This orogen is represented in Colombia by sedimentary and metasedimentary units of very-low-grade schists, migmatitic gneisses, paragneisses, and syntectonic and posttectonic granitoids (Mantilla et al., 2016; Rodríguez, 2022; Tazzo-Rangel et al., 2018; Van der Lelij et al., 2016), which reached the upper amphibolite and granulite facies at the top of the Famatinian Orogeny (~470 Ma) (Tazzo-Rangel et al., 2018; Zuluaga et al., 2017).

On this orogen, at the end of the Triassic and the beginning of the Jurassic (~214-184 Ma) (Rodríguez et al., 2017, 2019; Van der Lelij et al., 2016), magmatism that formed peraluminous, I- and S-type (López and Zuluaga, 2020; Rodríguez et al., 2017, 2019b, 2020; Zuluaga and López, 2019) batholithic bodies and stocks of predominantly monzogranitic to syenogranitic composition (Figure 2a) (Rodríguez et al., 2017, 2020a; Ward et al., 1973) developed in a more eastern position than the belts of the volcanic arcs of the Carboniferous (Leal Majía, 2011), Permian, and Lower to Middle Jurassic (Rodríguez et al., 2019, 2020a, 2020b) (Figure 2a and b).

3. Distribution of magmatic belts

The arc magmatic belts that are discussed in this article are mostly emplaced in the Chibcha Terrain, the Famatinian Oro-
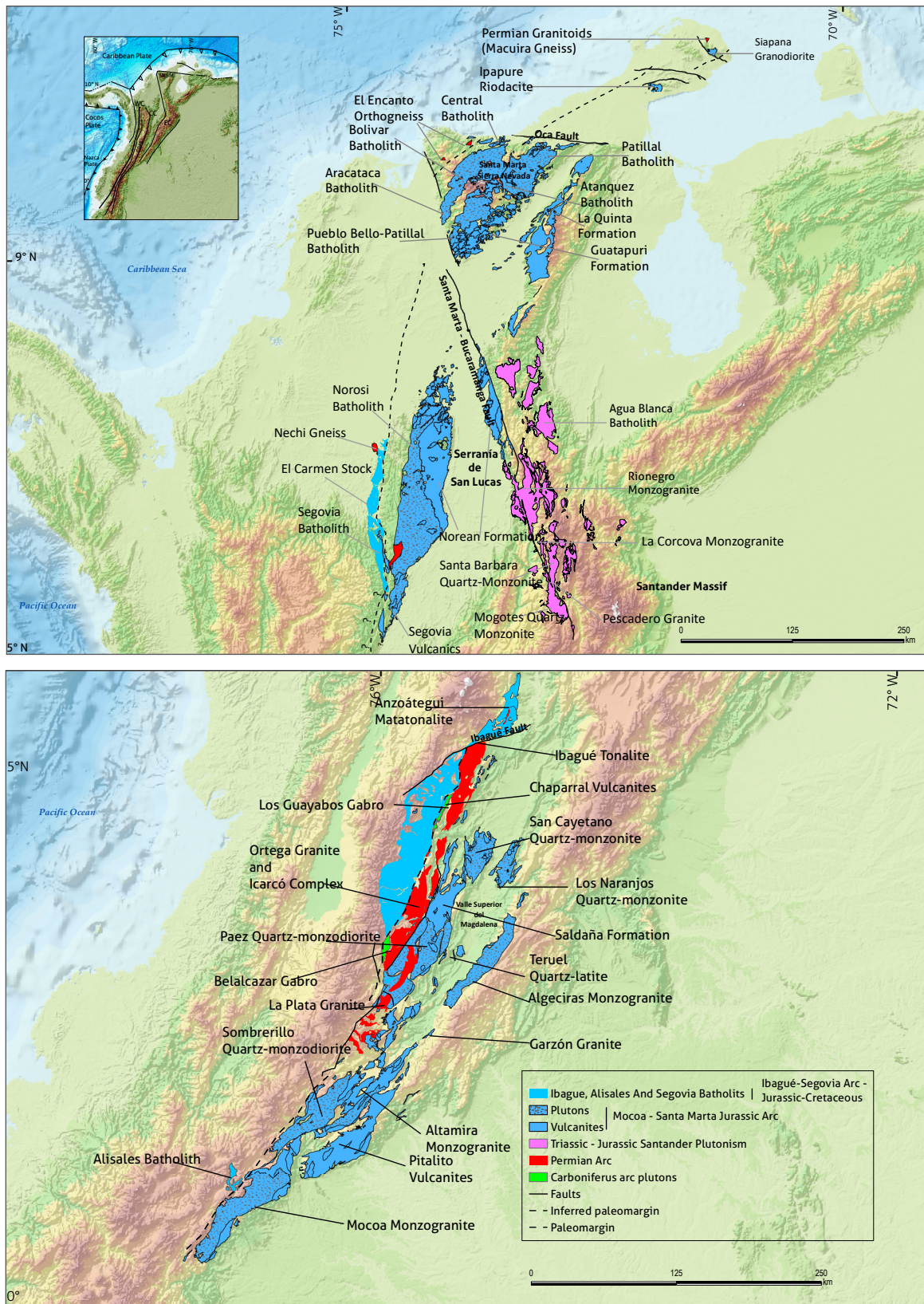
Figure 2. Distribution of the Carboniferous to Lower Cretaceous magmatic belts on the western margin of northern Gondwana in Colombia

gen, and to a lesser extent in the Tahamí and Anacona Terranes (Figure 1). These belts occupy part of the Central and Eastern cordilleras, the San Lucas range, the Sierra Nevada de Santa Marta, and La Guajira.

According to Restrepo and Toussaint (2020), the Chibcha Terrane mainly consists of a Grenvillian metamorphic basement (Stenian-Tonian) and Famatinian (Caledonian) low- to mid-grade metamorphic rocks. We consider the Andaqui Terrane of Restrepo and Toussaint (2020) part of the Chibcha Terrane, and we extracted the Famatinian Orogen (Santander, Floresta, and Quetame massifs). To the west, the limit of the Chibcha Terrane with the Tahamí and Anacona Terranes and the Tierradentro Orogen (which is described below), rather than the faults described by Restrepo and Toussaint (2020), corresponds to the undeformed pluton belts of the Carboniferous, Permian, and Early–Middle Jurassic continental margin arc magmatic cycles. These belts mark the limit of the western margin of Gondwana.

The Carboniferous rocks are distributed in a discontinuous belt of gabbros and tonalites, which currently crop out on the eastern slope of the Central Cordillera of Colombia. To the east of the Carboniferous rocks, also on the western margin of the Chibcha Terrane, a belt of batholiths and Permian stocks of varied composition (granites, granodiorites, diorites, quartz monzonites, and monzonites) was formed. Currently, the Permian plutons are dispersed along the western margin of the Chibcha Terrane, on the eastern slope of the Central Cordillera, in the San Lucas range, in the Sierra Nevada de Santa Marta, and in the La Macuira range. Some of the blocks to the north of the Ibagué fault are deformed and crop out next to metamorphic rocks of the Anacona and Tahamí Terranes identified by Restrepo and Toussaint (2020).

The batholiths and granitic stocks of the Santander massif, generated between the Late Triassic and Early Jurassic, crop out in the eastern part of the Famatinian Orogen in the eastern cordillera.

The belt of batholiths and stocks (monzodioritic, quartz monzodioritic and tonalitic) and volcanic and pyroclastic rocks formed between the Early Jurassic and the Middle Jurassic currently occupy a more eastern position than the Carboniferous and Permian plutons within the Chibcha Terrane, cropping out on both sides of the Upper Magdalena Valley, the Serranía de San Lucas, the Sierra Nevada de Santa Marta, the Serranía del Perijá, and in the Upper Guajira in the Serranía de Cosinas (Figure 1).

Of the belt of tonalitic to granodioritic batholiths and stocks formed from the Middle Jurassic to the Lower Cretaceous, some are in the suture, intruding the Anacona, Tahamí, and Chibcha Terranes. Others were emplaced within the Anacona and Tahamí Terranes, raising blocks of these two terrains that are conserved as roofs inside the plutons. The position of these plutons is more western than the belts of the Carboniferous, Permian, and Early to Middle Jurassic arcs. Currently, these plutons crop out in the axis and the eastern slope of the Central Cordillera and extend to the upper Guajira in the Serranía de La Macuira.

4. Materials and methods

For the development of this research, a regional sampling was made that included the Central Cordillera, upper Magdalena valley, Santander massif, Sierra Nevada de Santa Marta, Perijá range, and upper Guajira. The new data are integrated with results collected from previous works by the authors and others (Bustamante et al., 2010; Cuadros, 2012; Cuadros et al., 2014; González et al., 2015; Leal-Mejía, 2011; Quandt. et al., 2018; Villamizar et al., 2021; Zapata et al., 2016, among others). The geochemical and U–Pb geochronology data were grouped according to the correlation of units of each magmatic cycle.

4.1. Whole-rock geochemical analyses

We compiled whole-rock geochemical analyses of the units that make up each magmatic belt, from the Carboniferous to the Lower Cretaceous, and collected new data in the unknown units (Belalcázar and Los Guayabos gabbros). The whole-rock geochemical analyses were performed in the Laboratory of Analytical Geochemistry of the Servicio Geológico Colombiano, Bogotá headquarters. The major oxides and minor elements were analyzed with a Panalytical AXIOS Mineral X-ray fluorescence spectrometer. The former were quantified from samples fused with lithium metaborate and tetraborate, while the latter were quantified in pressed samples. For the analysis of trace elements, a mass spectrometer with inductively coupled plasma, Perkin Elmer NEXION, was used.

The geochemical diagrams were obtained using the GCD-kit *software* of Janoušek et al. (2006).

4.2. Geochronology

The geochronological analyses of the units that make up each magmatic belt from the Carboniferous to the Lower Creta-

ceous were compiled, and in some undescribed units, new U–Pb analyses were performed by laser ablation inductively coupled plasma–mass spectrometry (LA-ICP–MS) in zircon.

The new analyses were performed on rock chips that were crushed, pulverized, and sieved following the separation procedures of Castaño et al. (2018) and analyzed via LA-ICP–MS according to the procedures described in Peña et al. (2018). The zircons were concentrated in the Chemical Laboratory of the Servicio Geológico Colombiano, Medellín, using hydrodynamic and magnetic separation, although some samples were concentrated in the field by panning. Then, the crystals were selected manually with the help of an Olympus binocular magnifying glass in the Petrography Laboratory, Medellín headquarters. Cathodoluminescence (LC) images were acquired from the zircon grain mounts.

The analyses were performed in Photon Machines ablation equipment with a 193 nm excimer laser coupled to an Element 2 mass spectrometer. The isotopes used for manual integration were ^{238}U, ^{206}Pb, and ^{204}Pb. Plešovice (Sláma et al., 2008), FC-1 (Coyner et al., 2004), 91500 (Wiedenbeck et al., 1995, 2004), and Mount Dromedary (Renne et al., 1998) were used as reference standards. The spots analyzed in the zircons were 20 microns in diameter. Data reduction was performed using the Iolite v2.5® program in IGOR Pro 6.3.6.4® (Hellstrom et al., 2008; Paton et al., 2010). The correction for common lead was performed according to the evolution model of Stacey and Kramers (1975). The results correspond to the mean of the data obtained after applying data discrimination to two standard deviations.

5. Results

Figure 2 shows the current location of the magmatic belts defined by Rodríguez et al. (2019, 2020b), Leal et al. (2019), and

in the present work. The new ages obtained in this study are presented in Table 1. Supplementary Table TS1 summarizes the U–Pb data used to obtain the probability density plots of the magmatic cycles and presents 324 U–Pb ages in zircons obtained by different laboratories, mainly using LA-ICP–MS procedures, including the zircon ages of the nine rocks collected by the authors (Table 1) in regions without previous dating. Supplementary Table TS2 shows the chemical results, including the new analyses, which are used in the chemical classification diagrams of each magmatic cycle.

5.1. Geochronology

Los Guayabos and Belalcázar gabbros. Sample DAR-028 corresponds to a tonalite that outcrops near gabbro and gabbro breccia (composed of angular gabbro blocks of varied shapes and sizes surrounded by white leuco-tonalites). Sample WB-162 corresponds to a gabbro collected west of Belalcázar (Cauca). The zircons of sample DAR-028 are subhedral and euhedral prismatic, slightly pink, translucent, and *stubby*; some present inclusions, and most have fractured edges. In the CL image, the zircons have concentric zoning, in which the difference between the ages of the nucleus and the edges is approximately 10 Ma. The zircons of sample WB-162 are prismatic, colorless, and euhedral, with lengths between 100 and 200 μm and widths between 40 and 150 μm. In the CL images, it is possible to identify parallel banded linear textures in shades of light and dark gray (Figure 3).

For the calculation of the age of the DAR-028 sample, data with discordant values > 10% and precision errors > 5% were discarded. For the WD-162 sample, data with discordant values > 5% and precision errors > 3% were discarded. The average age for the DAR-028 sample was 317.2 ± 1.3 Ma (n = 58, MSWD = 2.4). The average age of the WB-162 sample was 325.9 ± 2.4 Ma (n = 42, MSWD = 3.3) (Figure 4). Both

Table 1. Carboniferous to Cretaceous U–Pb ages from rocks related to arc magmatic cycles

| Sample			Rock	Unity	U-Pb Age (Ma)	MSWD
WB-162	1122000	791840	Gabbro	Belalcázar gabbro	325.9 ± 2.4	3.3
DAR-028	935484	843111	Tonalite	Los Guayabos gabbro	317.2 ± 1.3	2.4
AMC-0194	1735620	1026510	Mylonitic orthogneiss	El Encanto orthogneiss	276.2 ± 1.3	2.0
GOE-1106A	1842115	971410	Mylonitic gneiss	Macuira gneiss	278.5 ± 1.8	3.3
GOE-1106B	1842066	971421	Monzogranite	Macuira gneiss	288.7 ± 1.5	2.7
JPZ-376	1157889	817853	Granodiorite	Páez quartz monzodiorite	184.7 ± 0.9	3.8
GOE-1127	1161083	826740	Monzogranite	Páez quartz monzodiorite	187.4 ± 1.7	2.9
MIA-684	1827161	974762	Granodiorite	Siapana granodiorite	166.5 ± 1.5	2.6
GR-6808	1036215	1734551	Pl-Hbl mylonitic gneiss	Buritaca gneiss	151.3 ± 3.6	2.7
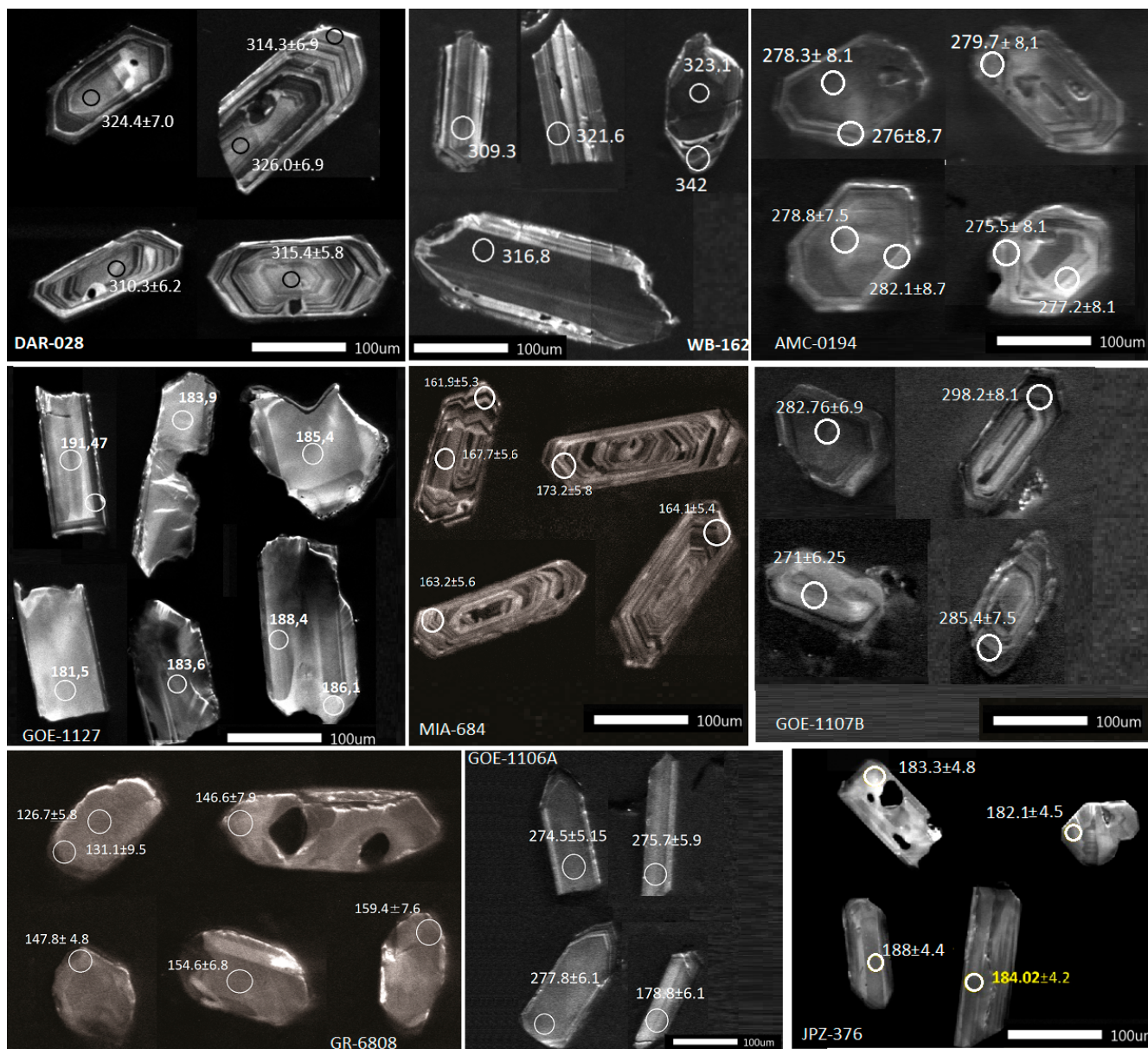
Figure 3. Representative cathodoluminescence images of zircon crystals of each dated sample

results are interpreted as crystallization ages with Th/U ratios between 0.2 and 1.7, typical of igneous zircons (Rubatto, 2002).

El Encanto orthogneiss and Permian ages in the Serranía de Macuira. Sample AMC-0194 corresponds to a plagioclase-quartz-amphibole-biotite-titanite mylonitic orthogneiss collected along the Buritaca-Guachaca road. The zircons are euhedral, colorless with a slight pale pink hue, generally without inclusions, with lengths between 80 × 150 μm and 100 × 200 μm,

indicating *short stalky* shapes. In the CL images, the crystals are prismatic with homogeneous gray nuclei and edges with concentric zoning in different shades of gray (Figure 3).

For the calculation of age, data with discordant values > 10% and precision errors > 5% were discarded. The average age calculated for the AMC-0194 sample is 276.2 ± 1.3 Ma (n = 101, MSWD = 2.0), which is interpreted as the age of rock crystallization, in which Th/U ratios vary between 1 and 3.1, typical for igneous zircons (Rubatto, 2002).
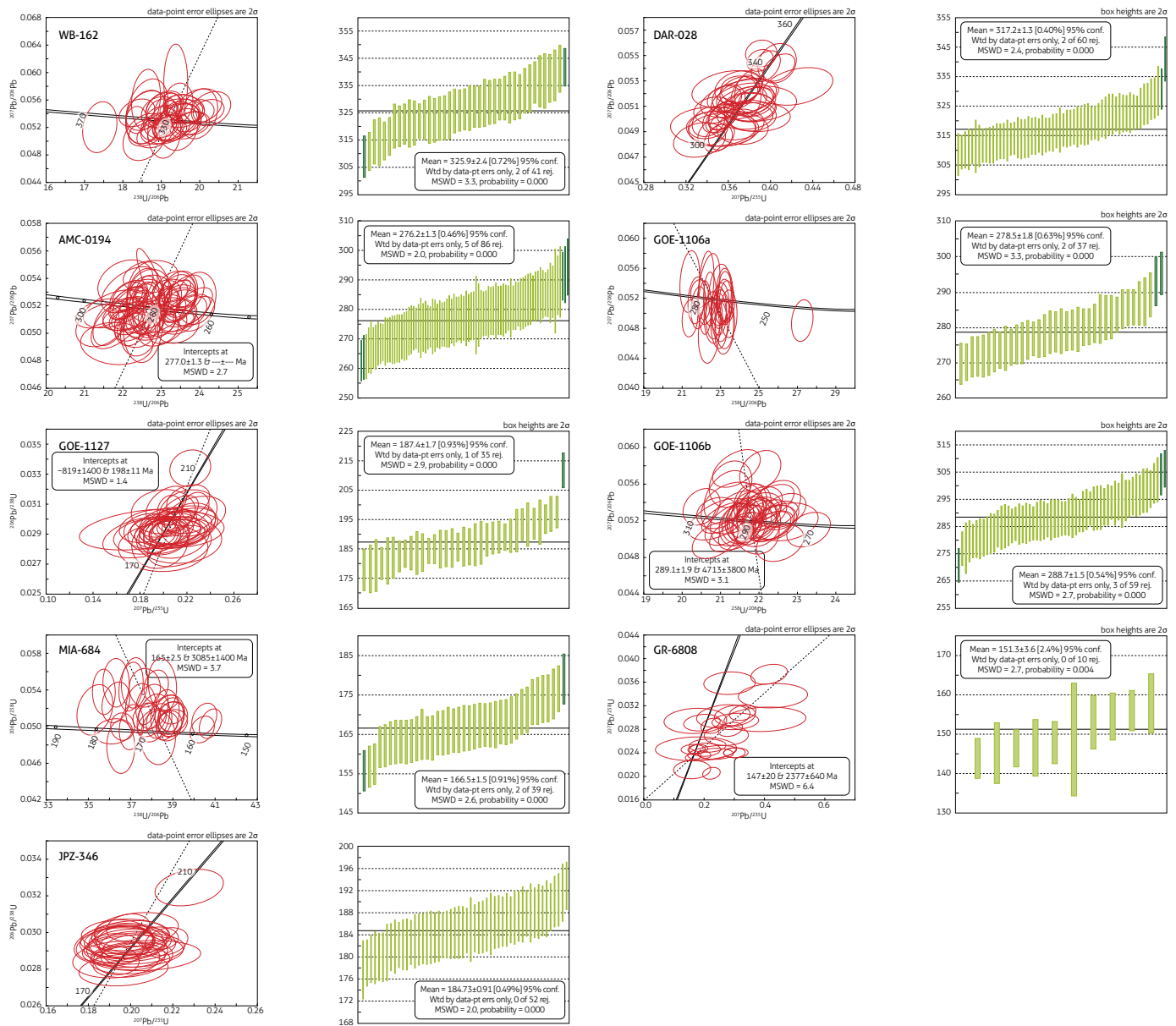
Figure 4. Wetherill and Tera-Wasserburg concordia diagrams and weighted mean age of the samples dated by the U-Pb method in zircon

In the Serranía de Macuira, two ages are calculated in rocks that are mapped as Macuira gneiss, corresponding to samples GOE-1106a and GOE-1106b, classified as a mylonitic granitoid and as a deformed monzogranite, respectively. The zircons of sample GOE-1106a are prismatic euhedral, stalky, and less frequently short euhedral crystals 80-120 μm in length. The zircons of sample GOE-1106b are colorless, stalky, and prismatic euhedral, with lengths of 80-120 μm. Some have inclusions, fractures, and surface oxides. In the CL images, the zircons of

sample GOE-1106a present homogeneous gray nuclei and thin edges with concentric or banded structures. The zircons of sample GOE-1106b present concentric structures in different shades of gray; some are microfractured and have few inherited xenocryst nuclei.

For the calculation of the ages of samples GOE-1106a and GOE-1106b, data with discordant values > 10% and precision errors > 5% were discarded. For the GOE-1106A sample, one concordant data point of 232.6 ± 5.1 Ma was discarded becau-

se it deviates from the main population with an average age of 278.5 ± 1.8 Ma (n = 37, MSWD = 3.3) (Figure 4). For the GOE-1106b sample, an average age of 288.7 ± 1.5 Ma (n = 59, MSWD = 2.7) was obtained (Figure 4). Both results are interpreted as crystallization ages and have Th/U ratios of 0.43 to 1.96 and 0.25 to 9.99, respectively.

Páez quartz monzodiorite. Sample JPZ-376 corresponds to a granodiorite that was collected in the Baché village of the municipality of Santa María (Huila), and sample GOE-1127 corresponds to a charnockite (mangerite) collected along the Planadas-Santa María road. The zircons of sample JPZ-376 are prismatic with euhedral shapes and sizes between 70 and 150 μm. In CL images, oscillatory zoning typical of igneous zircons, involute nuclei, and some with magmatic reabsorption edges are observed. In sample GOE-1127, the zircon crystals are prismatic euhedral with sizes > 100 μm, stalky to needle-shaped, generally fractured, and colorless. In the CL images, they present homogeneous nuclei with weak oscillatory zoning at the edges, some with a linear texture (Figure 2).

For the calculation of age, data with discordant values > 10% and precision errors > 5% were discarded. The average age calculated for the JPZ-346 sample was 184.7 ± 0.9 Ma (n = 53, MSWD = 3.8), with Th/U ratios between 0.55 and 1.27. The GOE-1127 sample yielded a weighted average age of 187.4 ± 1.7 Ma, with MSWD = 2.9 (Figure 4), and Th/U ratios between 0.99 and 1.70, corresponding to zircons formed in a magmatic chamber (Rubatto, 2002).

Siapana granodiorite. Sample MIA-684 is a granodiorite collected at El Tablazo-Siapana Hill in the Serranía de La Macuira.

The zircons are euhedral and stalky to columnar in shape; some are fractured, with few black inclusions. In the CL images, they present a concentric internal structure marked by changes in gray hue (Figure 3), typical of crystals generated in igneous environments.

For the calculation of the age of MIA-684, data with discordant values > 10% and precision errors > 5% were discarded. The average age calculated for the MIA-684 sample was 166.5 ± 1.5 Ma (n = 39, MSWD = 2.6) (Figure 4). The Th/U ratios varied between 0.11 and 0.77.

Buritaca gneiss. Sample GR-6808 was collected in the Buritaca gneiss unit on the road that borders the El Sol stream in the Sierra Nevada de Santa Marta and corresponds to plagioclase,

hornblende, and biotite mylonitic gneiss. The zircons are 50-100 μm, subhedral to euhedral, colorless, and stalky-short with oval to prismatic terminations.

In the CL images, the crystals present homogeneous color, incipient concentric and banded zoning, internal microfractures, and inclusions.

For the calculation of the age of GR-6808, data with discordant values > 10% and precision errors > 10% were discarded. In addition, two data points in a homogeneous zircon crystal of 126.7 ± 5.8 and 131.14 ± 9.5 Ma, one concordant and the other discordant, were discarded (Figures 3 and 4). The average age calculated for sample GR-6808, dating the crystal edges and nuclei, was 151.3 ± 3.6 Ma (n = 10, MSWD = 2.7), with Th/U ratios between 0.22 and 0.56, which are interpreted as zircons that formed in a magmatic chamber. A second population of inherited crystals yielded a weighted average age of 180.7 ± 6.0 Ma (n = 10, MSWD = 2.7), with a Th/U ratio between 0.11 and 0.37. The sample also presented inherited crystals with ages from the Triassic (202.99 ± 12.9 Ma and 228.8 ± 10.1 Ma, n = 3), Neoproterozoic (664.46 ± 4.8 Ma, 776.02 ± 47. 8 Ma, 853.48 ± 50.8 Ma, 910.34 ± 42.5 Ma and 918.44 ± 45.6 Ma), and Mesoproterozoic (1037.92 ± 47.7 Ma).

6. Discussion

6.1. Magmatic cycles, unit correlations, cycle composition, and spatial location

A magmatic cycle corresponds to the period of geological time that elapses during the initiation, development, and collapse of a continental margin arc, in which a belt of plutons and volcanic rocks is formed in a determined position and presents particular compositional characteristics. In this scenario, several magmatic cycles and pluton belts are generated from the same subduction zone.

The correlation of the plutons of each magmatic cycle is based on their location in relation to the paleomargin, their geochemical composition, and their crystallization age. The magmatic cycles are identified as peaks in the U–Pb probability density plots of the plutonic rocks (and, in some cases, the volcanic units). In addition, the general geochemical composition of the pluton belts that represent the magmatic cycle is shown.

6.2. Carboniferous (ca. 333 Ma to ca. 300 Ma)

The first products of continental margin arc magmatism in the western paleomargin of Gondwana occurred in the Carboni-
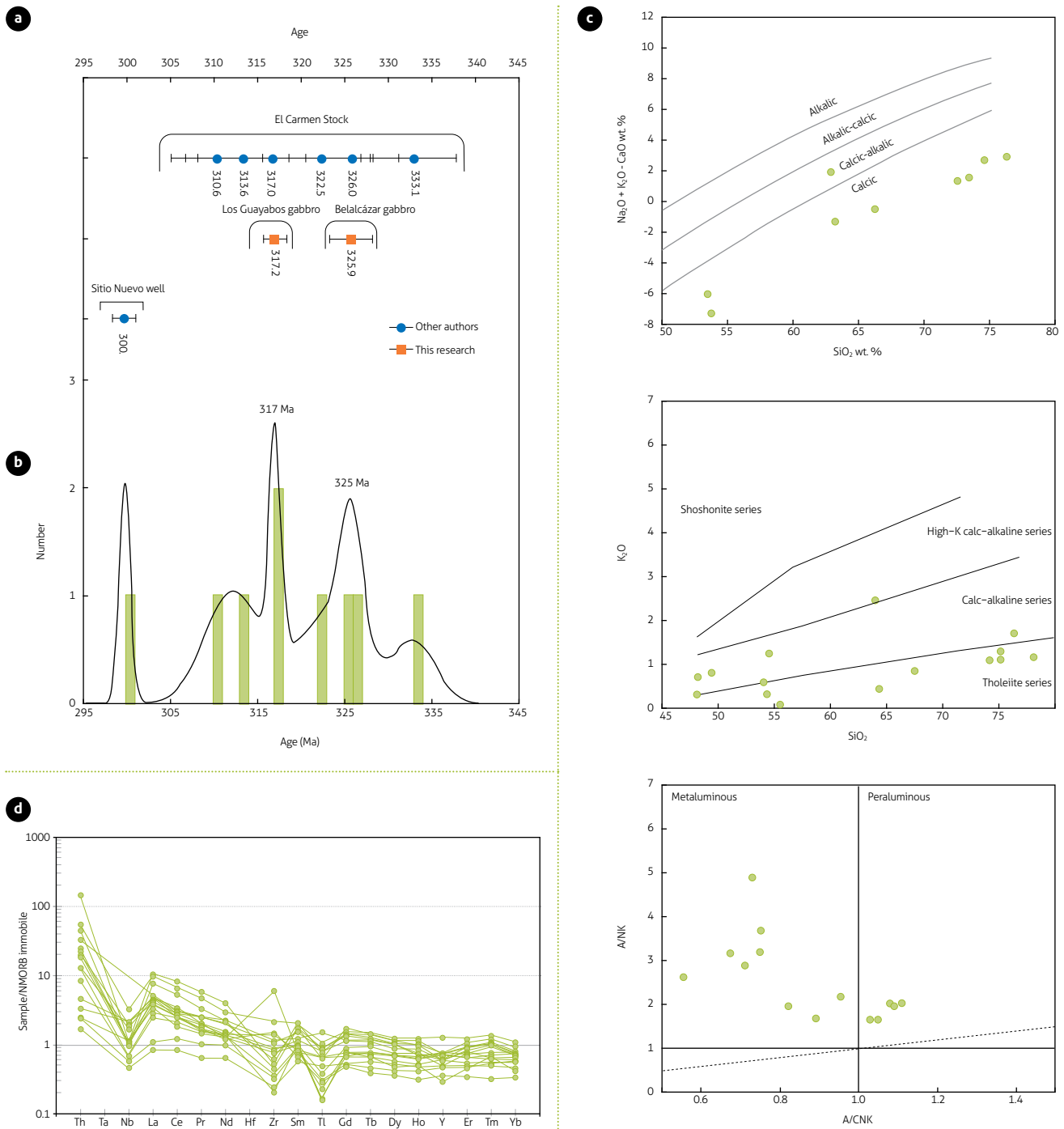
Figure 5. Age and composition of the plutons of the Carboniferous magmatic cycle
a) Correlation diagram of plutons of Carboniferous age; b) Diagram of probability density from the U–Pb ages of the plutons; c) Classification diagrams of carboniferous pluton samples; d) Diagram of immobile trace elements normalized to the normal mid-ocean ridge basalt (NMORB)

ferous from ca. 333 Ma to ca. 300 Ma (Leal Mejía, 2011; Leal Mejía et al., 2019; Rodríguez et al., 2019a). This magmatic record was recently discovered in the northern Andes, and thus

far, only the following bodies have been reported: the El Carmen stock (Leal Mejía, 2011) and Los Guayabos and Belalcázar gabbros (this work) in the Central Cordillera and a pyroxene

gabbro from the Sitio Nuevo-1 well in the lower Magdalena valley (Silva-Arias et al., 2016) (Figure 2).

The south to north geotectonic location of the Carboniferous plutons is as follows: the Belalcázar gabbro is located on the westernmost edge of the Gondwana paleomargin within the Neoproterozoic basement and is bound to the east by the Permian Ortega granite, and to the west, it is in faulted contact with the Upper Jurassic to Lower Cretaceous Ibagué batholith. The Los Guayabos gabbro outcrops farther north, in the same position related to the continental paleomargin. This unit is in faulted contact with Neoproterozoic metamorphic rocks and the Ibagué batholith to the west and in faulted contact with the Ibagué batholith and the Chaparral vulcanites to the east. The Chaparral vulcanites are from the Upper Jurassic and are located on the suture between the western margin of Gondwana and the metamorphic rocks previously described as Tierradentro gneisses and amphibolites. These latter rocks yielded Neoproterozoic maximum depositional ages in this sector and are older than the ages to the north of the Ibagué fault reported by Rodríguez et al. (2020a).

The El Carmen stock outcrops to the north of the Central Cordillera. This unit presents crystallization ages and compositions comparable to those of the Belalcázar and Los Guayabos gabbros. The El Carmen stock is located to the west of the Segovia batholith and is in faulted contact with the metamorphic rocks of the Cajamarca Complex (not yet dated in this sector) to the west of the Gondwana margin.

The ages of carboniferous magmatism vary between 333.1 ± 4.7 Ma and 300 ± 1.3 Ma and represent a magmatic cycle that lasted approximately 33 Ma, with two magmatic crystallization peaks ca. 325 Ma and ca. 317 Ma. The ages obtained for the Carboniferous plutons are shown in Figure 5a and Supplementary Table TS1.

The Carboniferous plutons are constituted by gabbros and I-type calcic leuco-tonalites (Figure 5b). The rocks are metaluminous and, to a lesser extent, peraluminous (in the most differentiated facies), presenting tholeiitic to calc-alkaline affinity (Figures 5c). The samples show Ba and Th enrichment, positive Pb anomalies, and negative Nb, Ti, and Zr anomalies (Figure 5d) related to magmas generated in subduction zones (Pearce, 2008), possibly in the first stages of continental margin arc magmatism.

The Carboniferous magmatic cycle is recorded in the zircons inherited in the Permian and Early Jurassic arc magmatic cycles (Figure 6), suggesting that these likely correspond to antecrysts or xenocrysts.

6.3. Permian to Triassic (ca. 300 Ma to ca. 234 Ma)

Following the Carboniferous magmatism, the second belt of continental arc plutons was emplaced on the Neoproterozoic basement of the western paleomargin of Gondwana during the Permian period (Figures 2 and 13). This cycle is represented by batholiths, stocks (La Plata and Ortega granites), igneous bodies with migmatitic structures (Icarcó Complex, parts of the La Plata Granite), and deformed mylonitic plutonic blocks (Nechí gneiss, El Encanto orthogneiss, and mylonites and deformed granites associated with the Macuira gneiss).

The latter rocks formed to the east of the continental margin of Gondwana; however, they are currently located to the west as deformed tectonic blocks. These rocks crop out along with rocks with Jurassic orogenic metamorphism and Triassic metamorphic blocks that are part of the collisional orogen (Tierradentro gneisses and amphibolites, the Cajamarca Complex, San Lorenzo schist, and La Macuira gneiss) (Blanco Quintero et al., 2014; Cardona et al., 2010; Piraquive, 2017; Rodríguez et al., 2020a; and this work).

The current location of each of the Permian plutons is to the east of the Carboniferous plutons (Figures 2 and 13). To the south, on the eastern flank of the Central Cordillera, the La Plata and Ortega granites and the Icarcó Complex are located within the western margin of Gondwana, in faulted contact to the east, and are intruded by plutons and vulcanites of the Early Jurassic (Mocoa-Santa Marta (AMSM) arc units; Rodríguez
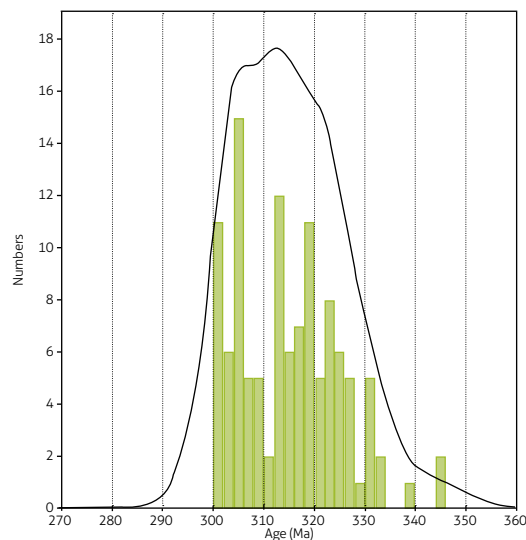

Figure 6. Probability density diagram based on inherited nuclei or zircons with Carboniferous ages obtained in the plutons of the Permian and Early to Middle Jurassic cycles
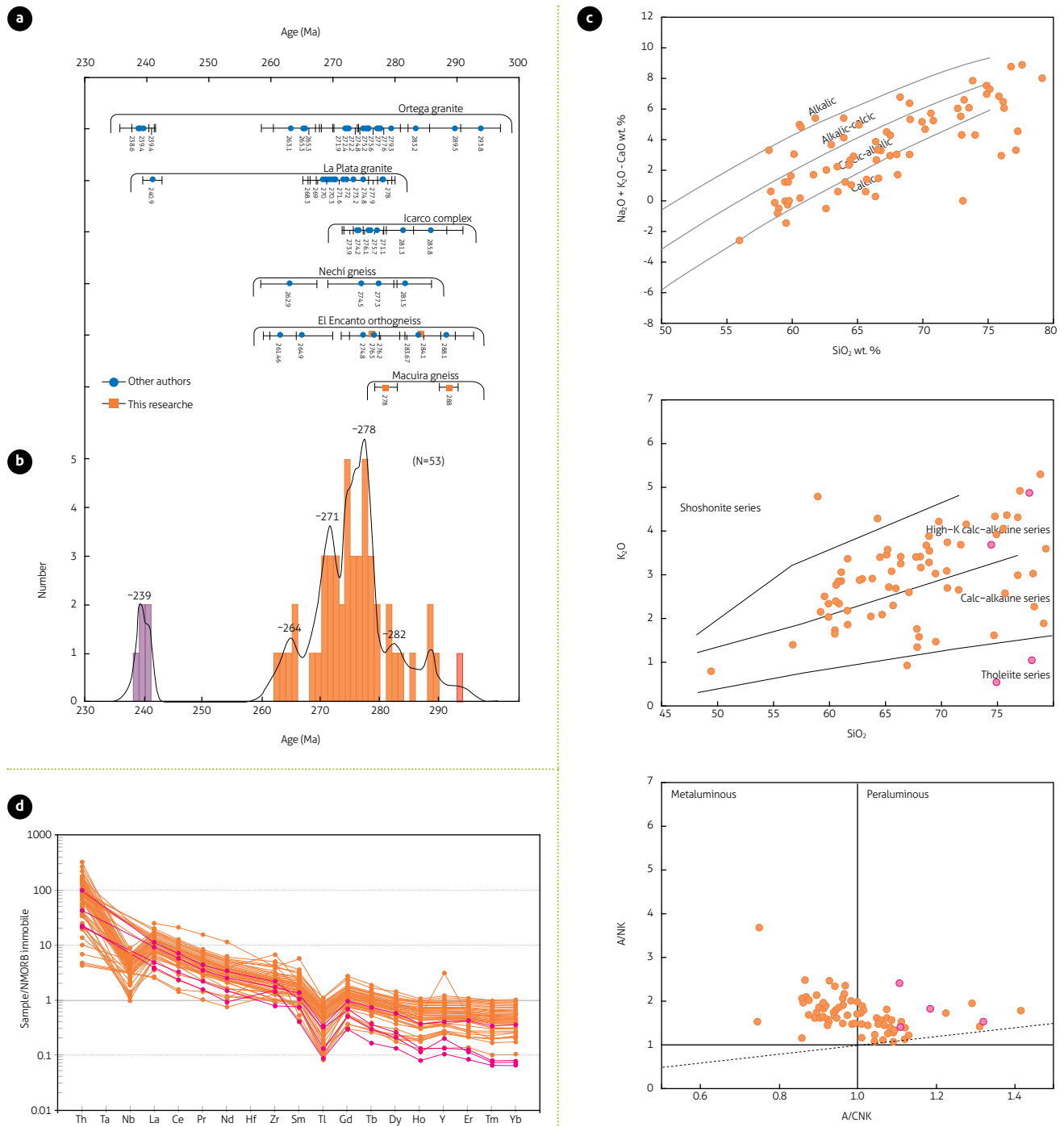
Figure 7. Age and composition of the plutons of the Permian and Triassic magmatic cycles
a) Correlation diagram of plutons of Permian and Triassic age; b) Diagram of probability density from the U–Pb ages of the plutons; c) Classification diagrams of Permian pluton samples with Triassic dikes; d) Diagram of immobile trace elements normalized to the NMORB

et al., 2019, 2020b). The Ortega granite and the Icarcó Complex, to the west, are in faulted contact with the Carboniferous Belalcázar gabbro and are intruded by the Late Jurassic to the Early Cretaceous Ibagué batholith. In addition, they were intruded by porphyritic subvolcanic bodies of the same age as the Ibagué batholith (Upper Jurassic-Lower Cretaceous).

To the north of the Ibagué fault, a deformed block of a Permian pluton appears as a mylonitic orthogneiss associated with the Triassic and Upper Jurassic Tierradentro Gneisses and Amphibolites unit (Bustamante et al., 2017; Rodríguez et al., 2020a).

The Nechí gneiss outcrops in the Serranía de San Lucas and corresponds to a granitoid with local mylonitic structures located to the west of the Segovia batholith and within metamorphic rocks of the Central Cordillera (Cajamarca Complex).

In the Sierra Nevada de Santa Marta, several deformed blocks of arc granitoids crop out, grouped under the name of El Encanto orthogneiss (Cardona et al., 2010; Piraquive, 2017), located next to Triassic and Jurassic metamorphic rocks. Finally, in the Serranía de Macuira, mylonites of igneous protolith and deformed granitoids are associated with the Macuira gneiss outcrop (this work).

The ages obtained for the Permian plutons are summarized in Figure 7 and Supplementary Table TS1. The geochronological record of this magmatism shows dates between 293.8 ± 3.8 Ma and 262.9 ± 4.5 Ma (ca. 30 Ma magmatic cycle). When analyzing the behavior of the entire magmatic belt of the Permian arc, at least four main magmatic crystallization events are recognized that can be grouped into four intervals: from 297 to 283 Ma, the beginning of plutonism; from 282 to 264

Ma, the development of the arc, with the highest crystallization peak ca. 278 Ma; from 264 to 257 Ma, the decay of crystallization and the final phase of pluton formation, with a discrete crystallization peak ca. 264 Ma. Finally, pink granite dikes and smaller bodies during a late intrusion event between ca. 245 and ca. 234 Ma occur (cycle of ca. 11 Ma), which yielded a crystallization peak ca. 239 Ma (Figures 7 and 8).

The composition of the plutons of this belt is heterogeneous: granites, granodiorites, diorites, quartz monzonites, and monzonites; some of them are deformed and have mylonitic foliation (Nechí gneiss, El Encanto orthogneiss, and mylonites and granitoids associated with Macuira gneiss). These plutons are distributed in the calcic field (calc-alkaline and alkali-calcic granitoids), are calc-alkaline and high-K calc-alkaline, I-type, and vary from metaluminous to peraluminous, with negative Nb and Ti anomalies typical of rocks generated in an arc continental margin environment.

The plutons and deformed granitoid bodies correspond to granites, granodiorites, diorites, quartz monzonites, and monzonites, which are distributed in the fields of calcic (calc-alkaline and alkalic-calcic) granitoids and in the calc-alkaline and high-K calc-alkaline fields (Figure 7).

The Triassic arc granites analyzed in this work have no genetic relationship with the S-type Triassic gneisses of the Central Cordillera, which were formed by crustal fusion and are emplaced in another continental block (Vinasco et al., 2006). These outcrops crop out in a more western position than the Carboniferous and Permian arc pluton belts.

Carboniferous and Permian arc magmatism cycles are recorded in inherited zircons from plutonic and volcanic rocks of Early to Middle Jurassic arc magmatism (Ramírez et al., 2020; Rodríguez et al., 2020b.) and the Mocoa-Santa Marta arc (AMSM) (Rodríguez et al., 2020b) (Figure 8), suggesting that this last cycle was emplaced in the Carboniferous and Permian pluton belts.

The zircons obtained in plutons and volcanic units from the Early to Middle Jurassic cycle of the AMSM record the inheritances of the Carboniferous, Permian, and Triassic magmatic cycles, as shown in Figure 8.

6.4. Triassic to Early Jurassic (ca. 234 to ca. 197)

Between 234 Ma (the last record of magmatic crystallization in dikes and smaller granite bodies associated with the plutons of the Permian arc) and ca. 197 Ma (beginning of the AMSM magmatic cycle; Rodríguez et al., 2020b), the accumulation of
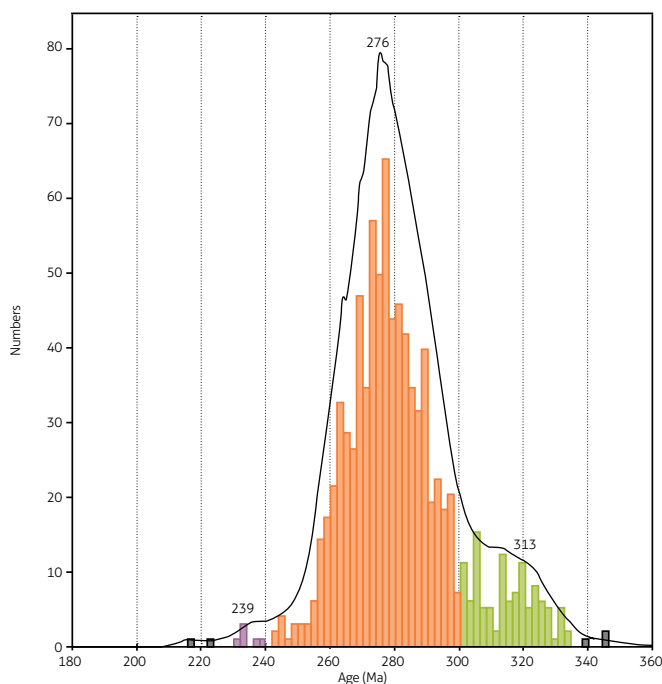

Figure 8. Probability density diagram for igneous ages obtained in inherited zircons in the plutons and volcanic rocks of the AMSM arc
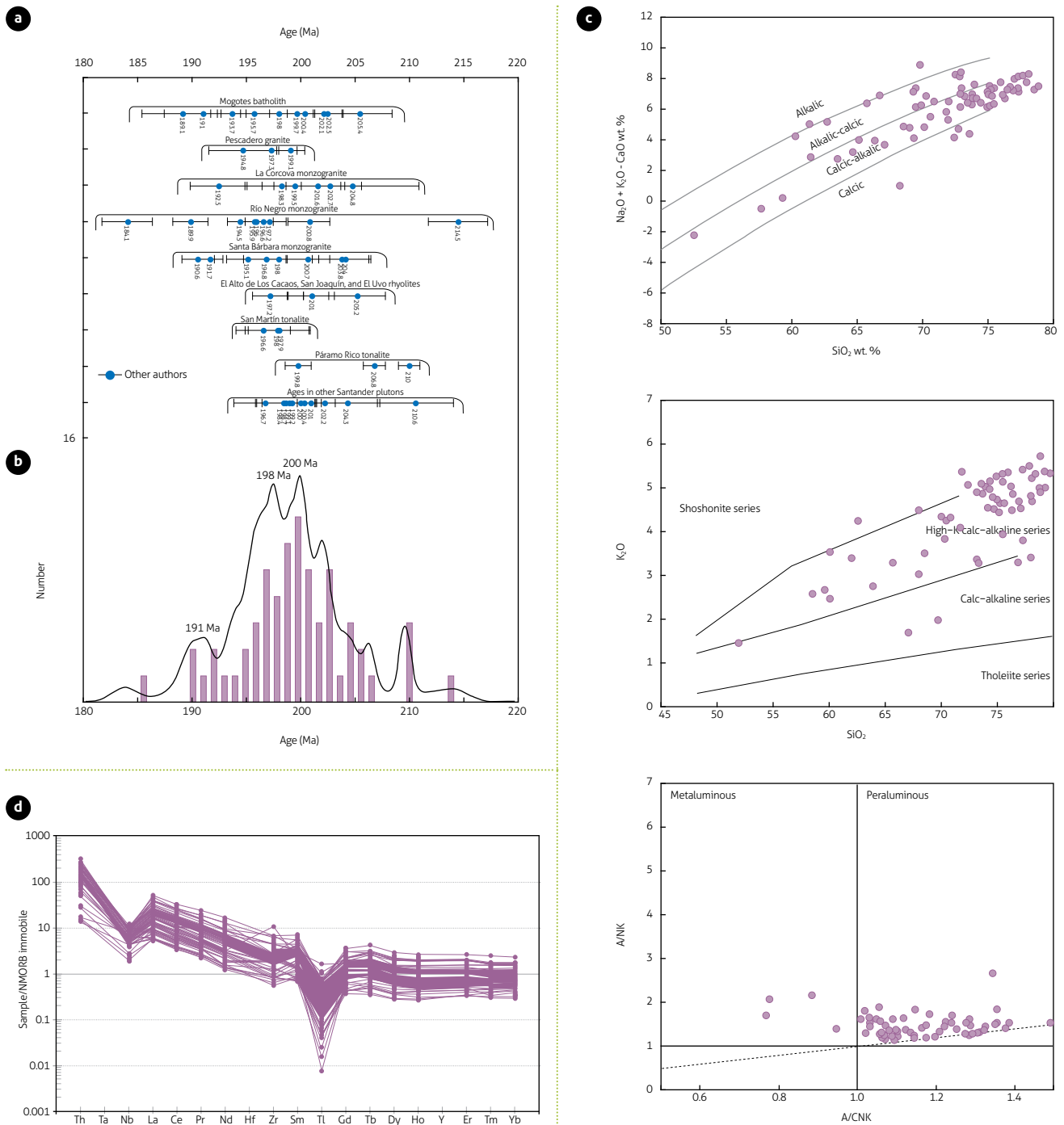
Figure 9. Age and composition of the plutons of the Triassic–Jurassic magmatic cycle of the Santander massif
a) Correlation diagram of plutons of Triassic–Jurassic age; b) Diagram of probability density from the U-Pb ages of the plutons; c) Pluton sample classification diagrams; d) Diagram of immobile trace elements normalized to NMORB

conglomerates, sedimentary breccias and subordinate shales, siltstones, and arkoses of the Luisa Formation is recorded in the western paleomargin of Gondwana (Cediel et al., 1980,

1981; Núñez and Murillo, 1982). The conglomerates and breccias are constituted by granitoid, gneiss, and granulite clasts, likely eroded from the Carboniferous and Permian arc plutons

formed in the margin and from rocks of the Neoproterozoic basement. The Luisa Formation rests discordantly on intrusive rocks with Permian crystallization ages (Ortega granite) and corresponds to the sedimentary record of the uplift and erosion period of the continental margin.

After the deposition of the Luisa Formation, discordant dark gray limestones of the Payandé Formation and minor intercalations of sandstones and lutites were deposited (Chicalá Member; Gómez, 2003). The latter record upper Triassic marine fauna (Geyer, 1973) and are related to a marine transgression event in the continental margin. The Payandé Formation would have been covered by volcanic material during the magmatic cycle that began in the Early Jurassic and extended until the Middle Jurassic (Montefrío sedimentites, Saldaña, Noreán, La Quinta formations, Sierra Nevada volcanic complex, and La Teta and Ipapure rhyodacites).

While erosion, sedimentation, and marine transgression occurred on the extinct plutons of the Carboniferous and Permian arcs (deposition of the Luisa and Payandé Formations) in the western paleomargin of Gondwana, back-arc magmatism began ca. 214 Ma, lasting until ca. 184 Ma (ca. 30 Ma magmatic cycle) (Figure 9). This belt is located within the Famatinian Orogen of the Santander massif in an eastern position in the interior of Gondwana (Figures 2 and 13).

This magmatism was characterized by the formation of batholiths and stocks of monzogranite composition, with subordinate granodiorites, syenogranites, and tonalites, from multiple magmatic pulses (Mogotes batholith; La Corcova, Santa Bárbara, and Río Negro monzogranites; Pescadero granite; and El Alto de Los Cacaos, San Joaquín, and El Uvo rhyolites, among others).

From a geochemical point of view, the rocks of this magmatism plot within the calc-alkaline and subordinate alkali-calcic granitoid fields (Figure 9c) of the high-K calc-alkaline series (Figure 9c) and are peraluminous (Figure 9c) and highly differentiated (Figure 9c), presenting negative Nb and Ti anomalies in the diagram of immobile trace elements normalized to normal mid-ocean ridge basalt (NMORB) (Figure 9d).

The ages obtained for the plutons and subvolcanic bodies are summarized in Figure 9a and Supplementary Table TS1. Analyzing the behavior of the Triassic–Jurassic magmatism of Santander reveals that during the entire magmatic cycle, predominantly monzogranitic rocks were formed, and each of the plutons was formed during an extended period of crystallization from multiple magmatic pulses (Rodríguez et al., 2020a,

2021). The cycle started ca. 214 Ma, with a progressive increase in magmatism and with the highest crystallization peak between ca. 200 and 198 Ma, decreasing the crystallization progressively until the end of the cycle ca. 184 Ma (Figure 9a).

These granitoids were generated by the fusion of rocks of the Paleozoic metamorphic basement of the Famatinian Orogen (Leal et al., 2019; López and Zuluaga, 2020; Rodríguez et al., 2017; Van der Lelij et al., 2016; Zuluaga and López., 2019), as suggested by the abundance of inherited zircons from the basement in these plutons (Rodríguez et al., 2020a) and the isotopic data (Leal et al., 2019; Van der Lelij et al., 2019).

The origin of this magmatism has been related to oblique subduction processes during the fragmentation of Pangea (López and Zuluaga, 2020; Rodríguez et al., 2017; Van der Lelij et al., 2016; Zuluaga and López, 2019) or partial fusion of the Santander massif metamorphic basement, thermally induced by the ascent of the mantle as a consequence of an extensional process, during the fragmentation of Pangea without being directly associated with subduction (Leal-Mejía et al., 2019).

Crustal thickness calculations based on Profeta et al. (2015) for Triassic–Jurassic granitoids of the Santander massif yielded values of approximately 60 km. These data indicate that the crust was thickened and could have delaminated.

Therefore, this study proposes another process that would also explain the fusion of continental crust in the Santander massif, corresponding to the delamination of the thickened lower eclogitic crust. This mechanism, like that of asthenospheric decompression by thinning of the crust, allows the incursion of mantle heat and induces extensive fusion of the continental crust (Thompson and Connolly, 1995).

6.5. Early Jurassic–Middle Jurassic (ca. 197 to ca. 164)

On the western margin of Gondwana, the magmatic activity of the arc returned in the Early Jurassic, ca. 197 Ma and continued until ca. 164 (magmatic cycle of ca. 33 Ma, Figures 10 and 11), forming large volumes of volcanic and plutonic rocks emplaced on the Neoproterozoic basement (AMSM; Rodríguez et al., 2020b) currently located on the eastern flank of the Central Cordillera, Upper Magdalena Valley, Serranía de San Lucas, Sierra Nevada de Santa Marta, and Upper Guajira (Figure 2).

During this period, explosive volcanic and subordinate lava deposits occurred along the arc axis (Saldaña, Noreán, and La Quinta formations; Pitalito vulcanites; Sierra Nevada de Santa Marta volcanic complex; and Ipapure-La Teta Hill rhyodacite). The magmatic cycle began with the crystallization of plutons
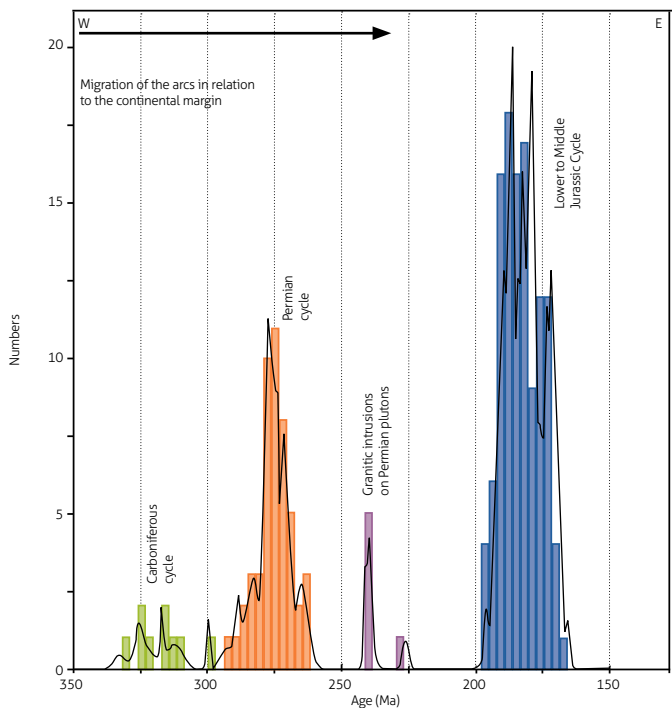
Figure 10. Magmatic arc cycles in the western margin of Gondwana between the Carboniferous and the Middle Jurassic

located to the east of the Carboniferous and Permian intrusive rocks (Sombrerillo quartz monzonite; Las Minas monzodiorite; El Astillero and Páez quartz monzodiorites; San Cayetano, Anchique, and Los Naranjos quartz monzonites; Dolores stock; Norosí granite; Guamocó granodiorite; Papayal monzonite; the Central batholith; and Ipapure granodiorite). This magmatism migrated to the east in the final stage of the arc cycle (Mocoa, Altamira, and Algeciras monzogranites; Garzón granite; Teruel quartz latite; and Pueblo Bello, Patillal, and Atánquez batholiths) (Figure 11).

The oldest Jurassic plutons of this cycle (located to the west) are metaluminous, and the youngest (located to the east) vary from metaluminous to peraluminous, indicating migration of magmatism in a west–east direction (Rodríguez et al., 2018, 2020b). The axis of the AMSM was located immediately to the east of the Carboniferous and Permian plutons, suggesting that the migration of the axis of the arcs between the Carboniferous and the Middle Jurassic occurred toward the interior of Gondwana in the same direction as the subduction of the Farallon Plate.

The first plutons of the AMSM, in southern Colombia, are located on the eastern flank of the Central Cordillera and Serranía de Las Minas. On their western edge, they intrude the Permian La Plata and Ortega granites, and toward the east, they intrude the Neoproterozoic basement of the Chibcha Terrane. To the north, in the Serranía de San Lucas, the plutons intrude the Neoproterozoic San Lucas gneiss, and in the Sierra Nevada de Santa Marta, they occupy the western flank, intruding the Neoproterozoic Los Mangos granulite and Buritaca gneiss.

The plutons of the AMSM are not deformed in the Serranía de San Lucas and the Sierra Nevada, as is the case with the granitoids of the Carboniferous and Permian arcs that were formed toward the edge in the western paleomargin of Gondwana.

When the AMSM migrated the plutonism toward the east, the pluton composition changed from tonalite and quartz monzonite to monzogranite (Rodríguez et al., 2018, 2020b). The later plutons crop out along the western flank of the Eastern Cordillera, upper Magdalena Valley, and eastern slope of the Sierra Nevada de Santa Marta, intruding the Neoproterozoic basement. These rocks partially cover or intrude the volcanic products of the same arc (Figure 2).

Between 197 and 184 Ma, coeval magmatism occurred in two different geotectonic positions in the interior of Gondwana: 1) the AMSM developed on the western flank of the Central Cordillera, Serranía de San Lucas, and the Sierra Nevada de Santa Marta; 2) back-arc magmatism developed in the Santander massif. Along the axis of the arc, I-type metaluminous plutonism and volcanism occurred, while in the back-arc, I- and S-type peraluminous plutonism, and probably volcanism, developed by crustal fusion in a radius of approximately 60 to 65 km, thickening the crust (calculated from La/Yb ratios) (Kay et al., 2014; Rodríguez et al., 2020a). In the back-arc, the magmatism ended ca. 184 Ma, while in the arc, it continued until ca. 164 Ma (Figures 9, 11, and 13).

The granitoids that constitute the AMSM cycle are calc-alkaline, with slight variations toward the alkali-calcic (Figure 11c); they belong to the high-K calc-alkaline series, and some are shoshonitic (Figure 11c). The oldest granitoids are metaluminous, and the youngest granitoids vary from metaluminous to peraluminous (Figure 11c), with negative Nb and Ti anomalies (Figure 11d).

The crystallization ages of the plutons of the AMSM vary between ca. 197 Ma and 164 Ma, with crystallization peaks at ca. 186 Ma, ca. 179 Ma, and ca. 170 Ma (Figure 11b).
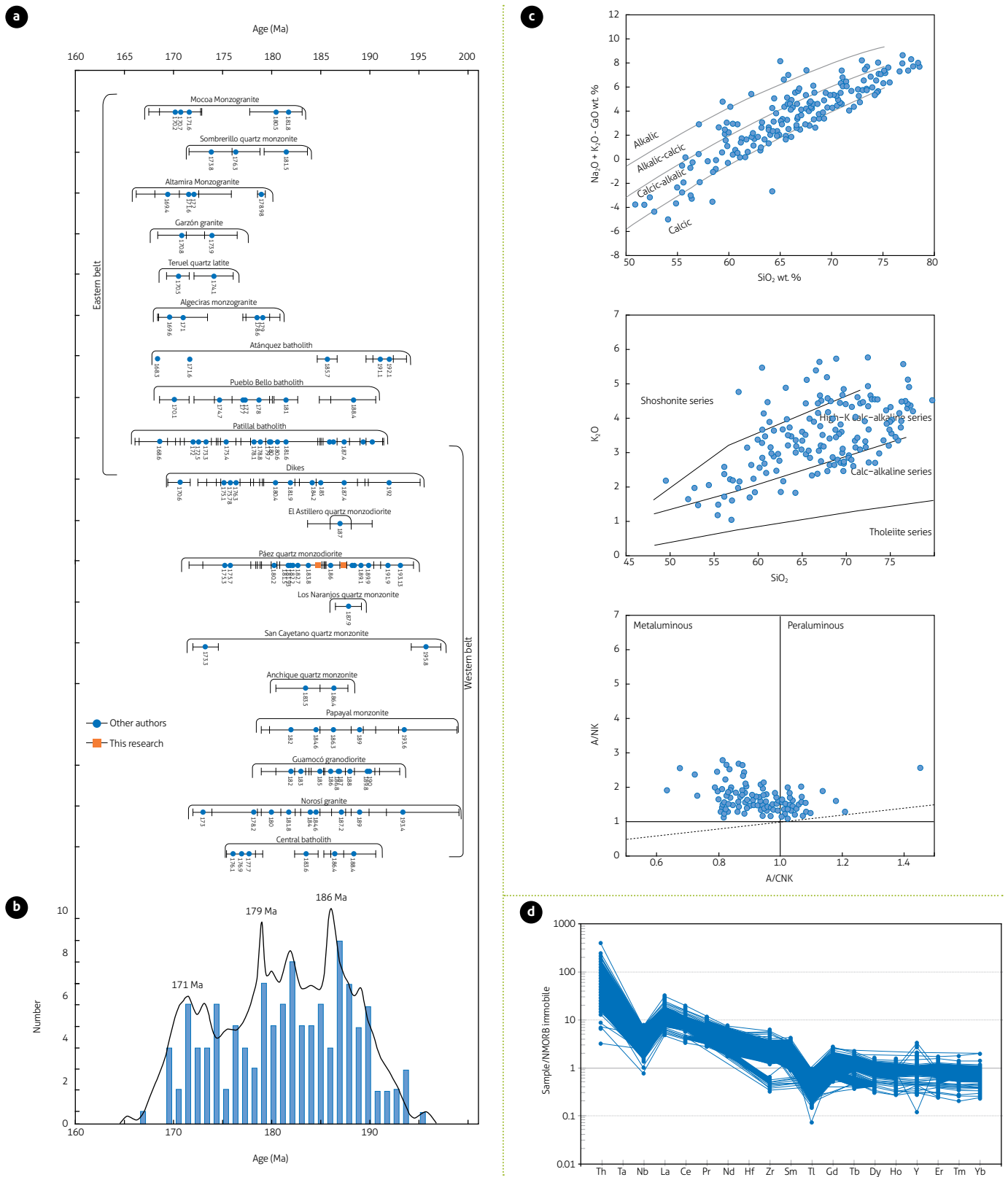
Figure 11. Age and composition of the plutons of the magmatic cycle of the lower to Middle Jurassic of the AMSM
a) Pluton correlation diagram; b) Diagram of probability density from the U–Pb ages of the plutons; c) Pluton sample classification diagrams; d) Diagram of immobile trace elements normalized to NMORB

6.6. Middle Jurassic to Lower Cretaceous (ca. 171 Ma and ca. 138 Ma)

Between ca. 171 Ma and ca. 138 Ma, several geological events occurred in the western paleomargin of Gondwana. Between 171 Ma and 164 Ma, magmatic activity occurred in two different geotectonic positions: 1) metaluminous and peraluminous monzogranite stocks and batholiths formed further into the interior of Gondwana on the western slope of the Eastern Cordillera and the eastern slope of the Sierra Nevada de Santa Marta during the final stages of the AMSM; 2) outside the western paleomargin of Gondwana, west of the Carboniferous, Permian, and Early to Middle Jurassic pluton belts, a new cycle of arc activity began in a basement composed of Ordovician and Triassic metamorphic rocks (Figures 2 and 13), traditionally called the Tahamí and Anacona Terranes (Restrepo and Toussaint, 2020) or the Cajamarca Complex (Maya and González., 1995). This new arc magmatism located to the west of the previous magmatic arcs is called the Ibagué-Segovia arc (AIS) (Rodríguez et al., 2020a, 2020b).

A third magmatic event corresponds to the formation of alkaline porphyry minor bodies composed of basaltic andesites that crystallized ca. 159 Ma. These rocks are located on the eastern slope of the Central Cordillera, intruding the plutons and volcanic rocks of the AMSM on the continental edge near the paleomargin (Rodríguez, 2018) (Figure 13).

The new magmatic cycle of the AIS is constituted by the Alisales, Ibagué, and Segovia batholiths, the Anzoátegui metatonalite, the Ibagué tonalite, the Payandé stock, and further north, the Siapana granodiorite (Figures 2 and 13). Plutonism was accompanied by explosive volcanism (Chaparral vulcanites: this work; La Malena volcanics and Segovia vulcanites: González et al., 2015) and began its magmatic activity ca. 171 Ma, ending ca. 138 Ma (magmatic cycle of ca. 33 Ma), with crystallization peaks at ca. 166 Ma, ca. 158.5 Ma, ca. 154 Ma and ca. 145 Ma (Figure 12b).

The plutons that are part of this cycle are constituted by tonalites and granodiorites with minor variations to quartz diorites and monzogranites. These rocks crop out adjacent to andesitic and dacitic vulcanite units and andesitic porphyry hypabyssal bodies that were formed in the final stage of the magmatic cycle. The porphyry bodies intrude the pluton belts formed in the Carboniferous and Permian cycles south of Ibagué.

The magmatism of the AIS coincides with the end of the AMSM magmatic cycle, the formation of metamorphic rocks against the continental paleomargin of Gondwana during the Late Jurassic, the amalgamation of new terranes at the margin, and the formation of subvolcanic bodies of alkaline basaltic andesites that are interpreted to be the result of the collapse and subsidence of the Farallon Plate in the mantle ca. 159 Ma (Rodríguez, 2018; Rodríguez et al., 2020b).

The magmatic cycle of the AIS extended before and after the collision of the Tahamí and Anacona Terranes against the Chibcha Terrain on the western margin of Gondwana. Locally, some plutons were emplaced in the suture (e.g., Ibagué Batholith), while others occupied positions within the amalgamated terranes and in metamorphic rocks formed during the collisional orogeny (e.g., Segovia and Alisales batholiths), intruding Ordovician, Triassic, and Jurassic metamorphic rocks (e.g., Perla gneiss: Ordovician; Tierradentro gneisses and amphibolites: Triassic and Jurassic ages; La Cocha-Río Téllez Complex: Upper Jurassic metamorphic and crystallization ages).

Plutons such as the Ibagué batholith and some subvolcanic porphyries intruded the plutons located within the Carboniferous, Permian, and Early to Middle Jurassic (AMSM) continental margins. In this period, the Anzoátegui metatonalite was probably deformed, developing foliation parallel to the Jurassic metamorphic rocks, while the Ibagué batholith presents only local deformation (Rodríguez et al., 2022).

The granitoids of the AIS cycle are mainly calcic, with some samples plotting in the calc-alkaline and alkali-calcic fields (Figure 12b). These rocks belong to the calc-alkaline series, and some belong to the high-K calc-alkaline series (Figure 12c). The granitoids are metaluminous and vary to peraluminous (Figure 11d), presenting negative Nb and Ti anomalies (Figure 12e).

6.7. Evolution of the margin and composition and development of the collisional orogen between 168 Ma and 154 Ma

The interpretation of the continental paleomargin of Gondwana has varied with the advancement of geological knowledge and the acquisition of more geochronological data. The continental paleomargin is considered the western limit of the Chibcha Terrane, although it has been modified. The continental boundary of the Chibcha Terrane corresponds to the Neoproterozoic basement and the undeformed pluton belts of the Carboniferous, Permian, and Early to Middle Jurassic arc cycles, which were emplaced in this basement (Rodríguez et al., 2019a). On the western side, against the continental boundary, the metamorphic sequences of the Ordovician (Anacona Terrane), Triassic (Tahamí Terrane), Late Jurassic (rocks with
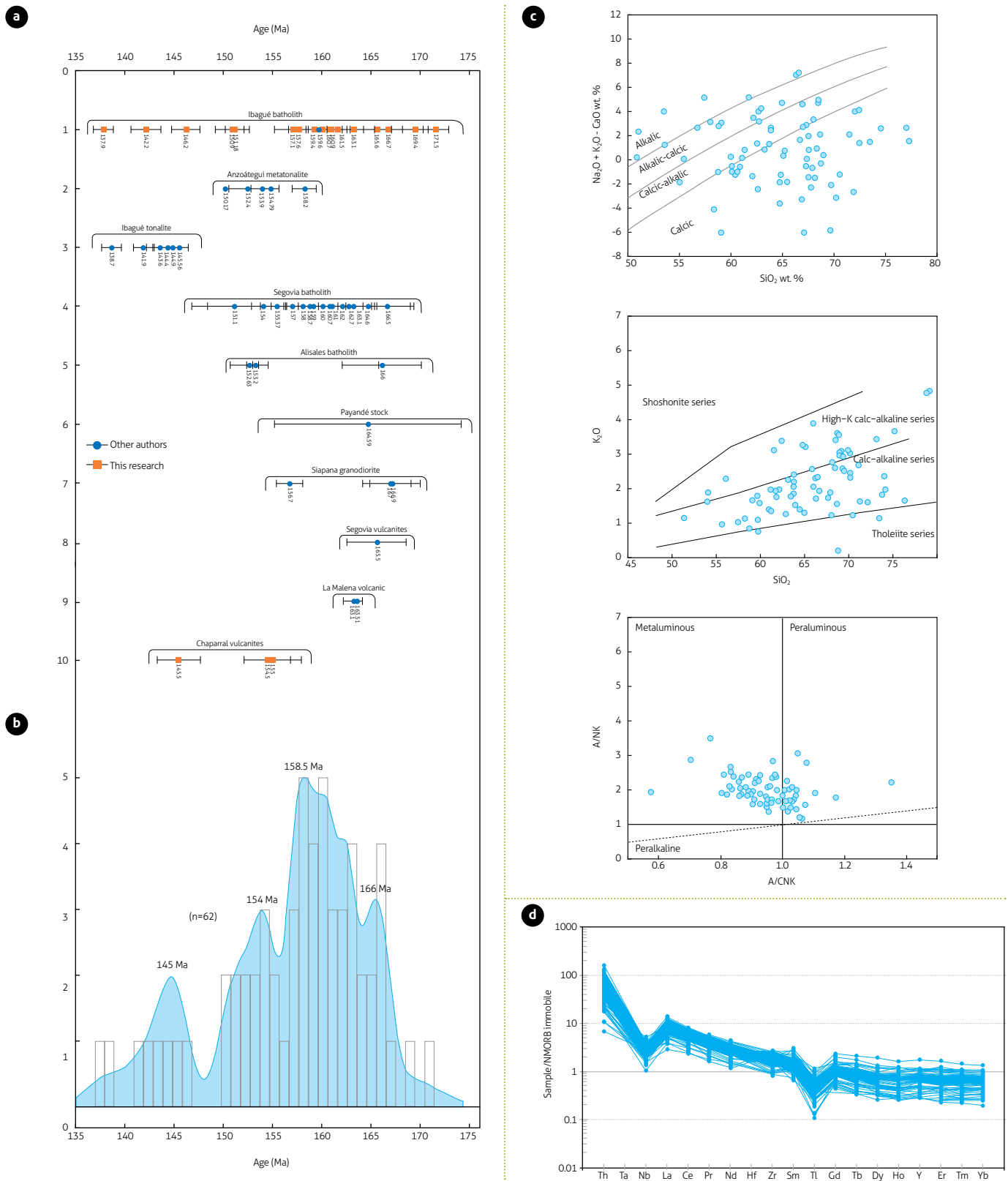
Figure 12. Age and composition of the plutons of the magmatic cycle from the Upper Jurassic to the Lower Cretaceous of the AIS
a) Pluton correlation diagram; b) Diagram of probability density from the U–Pb ages of the plutons; c) Pluton sample classification diagrams; d) Diagram of immobile trace elements normalized to NMORB

overlapping orogenic metamorphism), and deformed blocks detached from both margins, and rocks of oceanic crust crop out, marking the suture.

The subduction of the Farallon Plate between ca. 330 Ma and ca. 164 Ma likely partially eroded the continental paleomargin (hanging block), affecting the plutons formed during the Carboniferous and Permian magmatic cycles. Currently, deformed blocks of granitoids of the Permian cycle are present north of the Ibagué fault in the Serranía de San Lucas, Sierra Nevada de Santa Marta, and Upper Guajira (Permian orthogneiss in the Tierradentro gneisses and amphibolites: Bustamante et al., 2017; Nechí gneiss: Rodríguez and Zapata, 2017; El Encanto orthogneiss: Cardona et al., 2010 and Piraquive, 2017; and granites and mylonites of Permian age in the Macuira gneiss: this work), along with rocks with Triassic and/or Upper Jurassic metamorphism, interpreted as detached blocks that joined the amalgamated blocks during terrane collision. The erosion of the continental paleomargin, probably caused by subduction, was apparently lower south of the Ibagué fault, where the Carboniferous, Permian, and Early to Middle Jurassic pluton belts remain undeformed and inside the continental margin (Figure 2).

To the south of the Ibagué fault, the Ibagué batholith presents hanging roofs of the Ordovician metamorphic basement (La Perla gneiss) and the Triassic and Upper Jurassic Tierradentro gneisses and amphibolites, uplifted by the intrusion. In this sector, the Ibagué batholith and the Upper Jurassic subvolcanic bodies intrude the plutons of the Carboniferous, Permian, and Early to Middle Jurassic cycles on the eastern side of the suture.

Elsewhere in Colombia, the continental margin is limited on the western side by Upper Jurassic metamorphic rocks mixed tectonically with Triassic metamorphic rocks and Permian deformed plutonic blocks. This set of rocks is part of the collisional orogen located against the western paleomargin of Gondwana and was called the Tierradentro Terrane (Rodríguez et al., 2020a), but it is probably more accurate to consider it a collisional orogen that incorporates deformed blocks of both margins.

Orogenic metamorphism is present in units such as the Tierradentro gneisses and amphibolites (~167 to ~154 Ma; Rodríguez et al., 2017a, 2020a), the Cajamarca complex (~158 to ~147 Ma; Blanco-Quintero et al., 2014), La Cocha-Río Téllez complex (~163 Ma; Zapata et al., 2017), the metamorphic rocks of the Sierra Nevada de Santa Marta (Piraquive, 2017; this
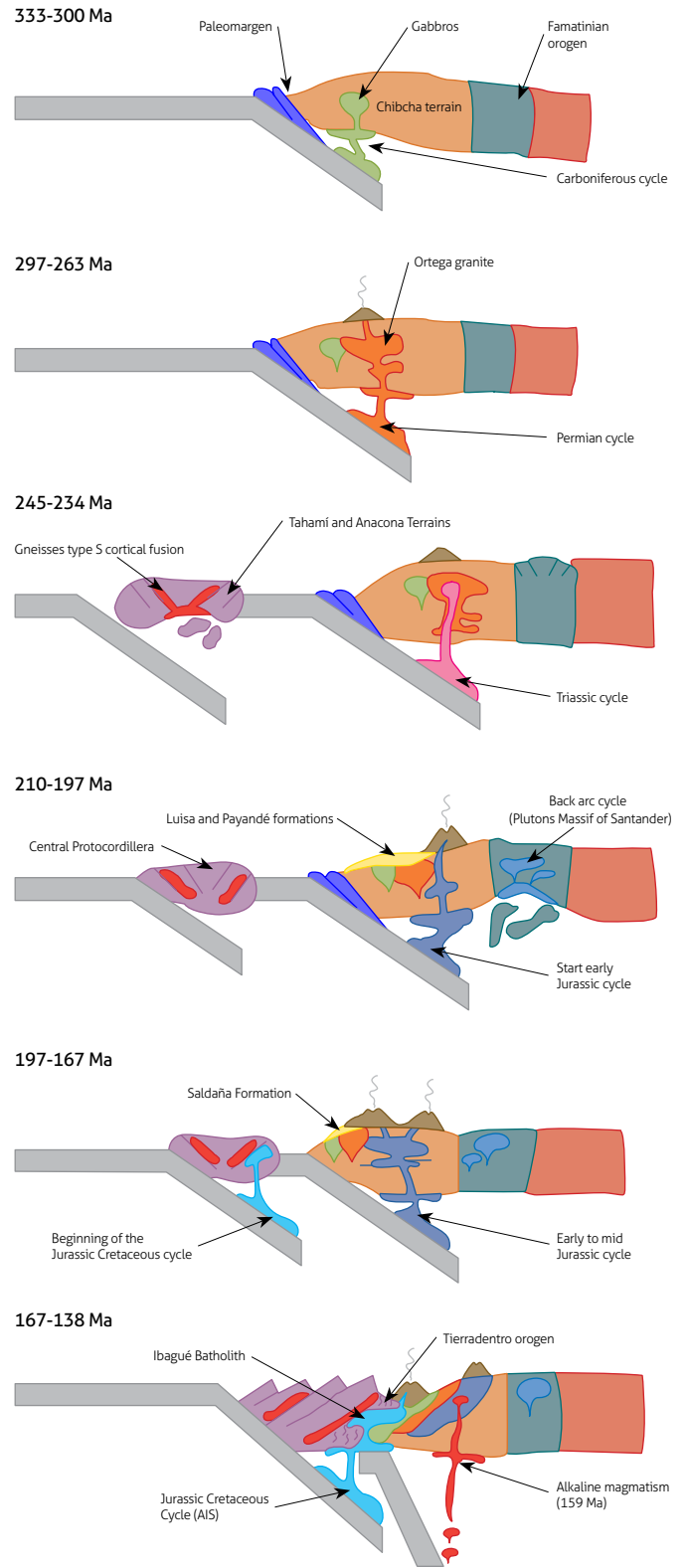

Figure 13. Tectonic reconstruction of the magmatic cycles between the Carboniferous and the Lower Cretaceous (330 to 138 Ma) in the northwestern paleomargin of Gondwana in Colombia

work), and most likely the Jarara and La Macuira ranges in the upper Guajira.

The rocks constituting the collisional orogen and the amalgamated blocks of the continental margin of Gondwana, immediately to the west of the continental paleomargin, vary in origin, age, and composition. These have been grouped into units and complexes (La Cocha - Río Téllez and Cajamarca complexes, Tierradentro gneisses and amphibolites, Davis gneiss, San Lorenzo schist, among others) and include amphibolites formed from arc metabasites and NMORB oceanic crust (Rodríguez et al., 2020a), serpentine blocks, metasediments, paragneisses, marbles, Permian mylonitic orthogneiss blocks, and AIS pluton intrusions. Some of these plutons were probably deformed during the collisional orogeny (Anzoátegui metatonalite: Rodríguez et al., 2020a). The first NMORB oceanic crustal rocks appear on the western side of the continental paleomargin and correspond to amphibolites and ultramafic blocks. Thus, the suture between the Chibcha and Tahamí-Anacona Terranes is a mixture of rocks of different origins, ages, and compositions.

Figure 13 summarizes the geotectonic evolution of the continental paleomargin of Gondwana between the Carboniferous and the Lower Cretaceous, following the known U–Pb geochronology data, the updated geology of the margin, and the whole-rock geochemistry of the magmatic cycles and metamorphic units located to the west of the paleomargin.

7. CONCLUSIONS

Each of the arc magmatic cycles that occurred in the western paleomargin of Gondwana between the Carboniferous and Middle Jurassic lasted approximately 30 to 35 Ma, except for the Triassic cycle, which lasted ca. 11 Ma.

The magmatic evolution between the Carboniferous and the Cretaceous shows a continuous compositional evolution between the continental margin arc cycles. In the Carboniferous, bodies of tholeiitic calcic gabbros and calc-alkaline tonalites predominate. In the Permian, calc-alkaline granites, granodiorites, diorites, quartz monzonites, and monzonites formed, with variations between the calcic and alkaline-calcic fields of the calc-alkaline to high-K calc-alkaline series. In the Early Jurassic, calc-alkaline quartz monzonites, quartz monzodiorites, monzodiorites, and tonalites of the high-K calc-alkaline series formed. At the end of the cycle, in the Middle Jurassic,

calc-alkaline and alkaline-calcic monzogranites and syenogranites of the high-K calc-alkaline series formed.

In the back-arc, the magmatic cycle lasted ca. 30 Ma, between ca. 214 Ma and ca. 186 Ma. The I- and S-type monzogranite and peraluminous syenogranite plutons formed during the entire cycle by crustal fusion. These rocks correspond to calc-alkaline to alkaline-calcic granites of the high-K calc-alkaline series.

At the end of the Jurassic, the intrusion of the AIS cycle began (ca. 171 Ma) outside the paleomargin in the Anacona and Tahamí Terranes, lasting ca. 33 Ma until the early Cretaceous (ended ca. 138 Ma). At the same time, the collision of the Anacona and Tahamí Terranes against the continental margin of Gondwana during the Late Jurassic (between ca. 167 Ma *and* ca. 154 Ma), and the collapse of the subduction zone that gave rise to the continental margin arc cycles of the Carboniferous, Permian, Triassic, and Early to Middle Jurassic occurred in the western margin of Gondwana. This latter collapse episode is marked by the intrusion of alkaline basaltic andesite bodies ca. 159 Ma.

The new zircon U–Pb age results presented in this study reveal two new Carboniferous gabbro bodies located on the eastern slope of the Central Cordillera. These new data improve the information and distribution of the Carboniferous magmatism of Colombia, previously included as part of the Ibagué batholith. In addition, in the upper Guajira, the first data of deformed granitoids of Permian age are obtained, extending the record of this magmatic cycle to northern Colombia.

REFERENCES

Álvarez, J. (1983). Geología de la cordillera Central y el occidente colombiano y petroquímica de los intrusivos granitoides meso-cenozoicos. *Boletín Geológico*, *26*(2), 1-175. https://doi.org/10.32685/0120-1425/bolgeol26.2.1983.53

Álvarez, M. J. (2013). *Petrología, geoquímica isotópica e metalogenia dos depósitos de ouro El Silencio e La Gran Colômbia, Distrito Mineiro Segovia–Remedios, Colômbia* [Master thesis]. Universidade de Brasilia, Brasilia.

Arango, M. I., Rodríguez, G., Zapata, G., & Correa Martínez, A. M. (2020). Monzogranito de Rionegro. In *Catálogo de las unidades litoestratigráficas de Colombia: Macizo de Santander* (Vol. 1). Servicio Geológico Colombiano. https://doi.org/10.32685/9789585279445-5-5

Arango, M. I., Rodríguez, G., Zapata, G., & Bermúdez, J. G. (2022a). Monzogranito de Mocoa. In *Catálogo de las unidades litoestratigráficas de Colombia: Valle Superior del Magdalena* (Vol. 2). Servicio Geológico Colombiano. https://doi.org/10.32685/9789585313194.1

Arango, M. I., Rodríguez, G., Bermúdez, J. G., & Zapata, G. (2022b). Monzodiorita de Las Minas. In *Catálogo de las unidades litoestratigráficas de Colombia: Valle Superior del Magdalena* (Vol. 2). Servicio Geológico Colombiano. https://doi.org/10.32685/9789585313194.4

Arango, M. I., Rodríguez, G., Bermúdez, J. G., & Zapata, G. (2022c). Cuarzomonzonita de Anchique. In *Catálogo de las unidades litoestratigráficas de Colombia: Valle Superior del Magdalena* (Vol. 2). Servicio Geológico Colombiano. https://doi.org/10.32685/9789585313194.7

Arango, M. I., Rodríguez, G., Zapata, G., & Bermúdez, J. G. (2022d). Cuarzolatita de Teruel. In *Catálogo de las unidades litoestratigráficas de Colombia: Valle Superior del Magdalena* (Vol. 2). Servicio Geológico Colombiano. https://doi.org/10.32685/9789585313194.9

Arango, M. I., Rodríguez, G., Zapata, G., & Bermúdez, J. G. (2022e). Monzogranito de Altamira. In *Catálogo de las unidades litoestratigráficas de Colombia: Valle Superior del Magdalena* (Vol. 2). Servicio Geológico Colombiano. https://doi.org/10.32685/9789585313194.12

Bayona, G., García, D., & Mora, G. (1994). La Formación Saldaña: producto de la actividad de estratovolcanes continentales en un dominio de retroarco. In F. Etayo-Serna (ed.), *Estudios geológicos del Valle Superior del Magdalena*. Universidad Nacional de Colombia.

Bayona, G., Jiménez, G., Silva, C., Cardona, A., Montes, C., Roncancio, J., & Cordani, U. (2010). Paleomagnetic data and K-Ar ages from Mesozoic units of the Santa Marta massif: A preliminary interpretation for block rotation and translations. *Journal of South American Earth Sciences*, *29*(4), 817-831. https://doi.org/10.1016/j.jsames.2009.10.005

Blanco-Quintero, I. F., García-Casco, A., Toro, L. M., Moreno, M., Ruiz, E. C., Vinasco, C. J., Cardona, A., Lázaro, C., & Morata, D. (2014). Late Jurassic terrane collision in the northwestern margin of Gondwana (Cajamarca complex, eastern flank of the Central Cordillera, Colombia). *International Geology Review*, *56*(15), 1852-1872. https://doi.org/10.1080/00206814.2014.963710

Bermúdez, J. G, Zapata, G., Rodríguez, G., & Arango, M. I. (2022a). Cuarzomonzonita de Sombrerillo. In *Catálogo de las unidades litoestratigráficas de Colombia: Valle Superior del Magdalena* (Vol. 2). Servicio Geológico Colombiano. https://doi.org/10.32685/9789585313194.2

Bermúdez, J. G., Arango, M. I., Rodríguez, G., & Zapata, G. (2022b). Cuarzomonzonita de San Cayetano. In *Catálogo de las unidades litoestratigráficas de Colombia: Valle Superior del Magdalena* (Vol. 2). Servicio Geológico Colombiano. https://doi.org/10.32685/9789585313194.8

Bustamante, C., Cardona, A., Bayona, G., Mora, A., Valencia, V., Gehrels, G., & Vervoort, J. (2010). U-Pb LA-ICP-MS geochronology and regional correlation of Middle Jurassic intrusive rocks from the Garzon Massif, upper Magdalena valley and Central Cordillera, southern Colombia. *Boletín de Geología*, *32*(2), 93-109.

Bustamante, C., Archanjo, C., Cardona, A., & Vervoort, J. (2016). Late Jurassic to Early Cretaceous plutonism in the Colombian Andes: a record of long-term arc maturity. *GSA Bulletin*, *128*(11-12), 1762-1779. https://doi.org/10.1130/B31307.1

Bustamante, C., Archanjo, C. J., Cardona, A., Bustamante, A., & Valencia, V. A. (2017). U-Pb ages and Hf isotopes in zircons from parautochthonous mesozoic terranes in the western margin of Pangea: implications for the terrane configurations in the northern Andes. *The Journal of Geology*, *125*(5), 487-500. https://doi.org/10.1086/693014

Cardona, A., Cordani, U., & MacDonald, W. D. (2006). Tectonic correlations of pre–Mesozoic crust from the northern termination of the Colombian Andes, Caribbean region. *Journal of South American Earth Sciences*, *21*(4), 337-354. https://doi.org/10.1016/j.jsames.2006.07.009

Cardona, A., Valencia, V., Garzón, A., Montes, C., Ojeda, G., Ruiz, J., & Weber, M. (2010). Permian to Triassic I to S-type magmatic switch in the northeast Sierra Nevada de Santa Marta and adjacent regions, Colombian Caribbean: Tectonic setting and implications within Pangea paleogeography. *Journal of South American Earth Sciences*, *29*(4), 772-283. https://doi.org/10.1016/j.jsames.2009.12.005

Castaño, J. M., Rodríguez F., & García, C. A. (2018). Caracterización de parámetros en la concentración de circones para andesitas, monzogranitos, riolitas, cuarcitas y cuar-

zomonzonitas. *Boletín Geológico*, (44), 25-38. https://doi.org/10.32685/0120-1425/boletingeo.44.2018.6

Cediel, F., Mojica, J., & Macías, C. (1980). Definición estratigráfica del Triásico en Colombia, Suramérica. Formaciones Luisa, Payandé y Saldaña. *Newsletters on Stratigraphy*, *9*(2), 73-104. https://doi.org/10.1127/nos/9/1980/73

Cediel, F., Mojica, J., & Macías, C. (1981). Las Formaciones Luisa, Payandé, Saldaña sus columnas estratigráficas características. *Geología Norandina*, (3), 11-20.

Cochrane, R. S. (2013). *U-Pb thermochronology, geochronology and geochemistry of NW South America: Rift to drift transition, active margin dynamics and implications for the volume balance of continents* [Ph.D. thesis]. University of Geneva, Switzerland. https://doi.org/10.13097/archive-ouverte/unige:30029

Cordani, U. G., Fraga, L. M., Reis, N., Tassinari, C. C. G., & Brito-Neves, B. B. (2010). On the origin and tectonic significance of the intra-plate events of Grenvillian-type age in South America: a discussion. *Journal of South American Earth Sciences*, *29*(1), 143-159. https://doi.org/10.1016/j.jsames.2009.07.002

Correa-Martínez, A. M., Rodríguez, G., Arango, M. I., & Zapata-García, G. (2019). Petrografía, geoquímica y geo cronología U-Pb de las rocas volcánicas y piroclásticas de la Formación Noreán al NW del Macizo de Santander, Colombia. *Boletín de Geología*, *41*(1), 29-54. https://doi.org/10.18273/revbol.v41n1-2019002

Correa Martínez, A. M., Ramírez, D., Rodríguez, G., Zapata, J. P., Obando, G., Muñoz, J. A., Rayo, L. del P., & Ureña, C. l. (2020). *Batolito Central de la Sierra Nevada, Magdalena, La Guajira y Cesar*. Servicio Geológico Colombiano.

Correa Martínez, A. M., Rodríguez, G., Arango, M. I., Zapata, G., & Bermúdez, J. G. (2020a). Batolito de Mogotes. In *Catálogo de las unidades litoestratigráficas de Colombia: Macizo de Santander* (Vol. 1). Servicio Geológico Colombiano. https://doi.org/10.32685/9789585279445.1

Correa Martínez, A. M., Rodríguez, G., Bermúdez, J. G., Arango, M. I., & Zapata, G. (2020b). Riolitas del Alto Los Cacaos. In *Catálogo de las unidades litoestratigráficas de Colombia: Macizo de Santander* (Vol. 1). Servicio Geológico Colombiano. https://doi.org/10.32685/9789585279445.9

Coyner, S. J., Kamenov, G. D., Mueller, P. A., Rao, V., & Foster, D. A. (2004). *FC-1: a zircon reference standard for the determination of Hf isotopic compositions via laser ablation ICP-MS*. American Geophysical Union, Fall Meeting. San Francisco, USA.

Cuadros, F. A. (2012). *Caracterização geoquímica e geocronológica do embasamento mesoproterozóico da parte norte da serrania de San Lucas (Colômbia)* [Master Thesis]. Universidade de Brasília.

Cuadros, F. A., Botelho, N. F., Ordónez-Carmona, O., & Matteini, M. (2014). Mesoproterozoic crust in the San Lucas Range (Colombia): An insight into the crustal evolution of the northern Andes. *Precambrian Research*, *245*, 186-206. https://doi.org/10.1016/j.precamres.2014.02.010

Frantz, J. C., Ordóñez, O., & Chemale, F. (2007). *Caracterización de ambientes geológicos con mineralizaciones de oro en los Andes colombianos* [Memories]. VIII Congreso Colombiano de Minería, Medellín.

González, H., Maya, M., Tabares, L. F., Montoya, A., Palacio, A. F., Sánchez, C., Barajas, A., & Vélez, W. (2015a). Memoria explicativa: Plancha 118 San Francisco. Scale 1:100 000. Servicio Geológico Colombiano.

González, H., Maya, M., García, J. F., Gómez, J. P., Palacio, A. F., & Vélez, W. (2015b). Memoria explicativa: Plancha 84 Los Canelos. Scale 1:100 000. Servicio Geológico Colombiano.

González, H., Maya, M., García, J. F., Camacho, J. A., Gómez, J. P., Cardona, O. D., Palacio, A. F., & Vélez, W. (2015c). Memoria explicativa: Plancha 94 El Bagre. Scale 1:100 000. Servicio Geológico Colombiano.

Hellstrom, J., Paton, C., Woodhead, J. D., & Hergt, J. M. (2008). Iolite: software for spatially resolved LA-(quad and MC) ICP-MS analysis. In P. Sylvester (Ed.), *Laser Ablation ICP–MS in the Earth Sciences: Current Practices and Outstanding Issues* (pp. 343-348). Mineralogical Association of Canada.

Ibáñez-Mejía, M., Ruiz, J., Valencia, V. A., Cardona, A., Gehrels, G. E., & Mora, A. R. (2011). The Putumayo Orogen of Amazonia and its implications for Rodinia reconstructions: New U–Pb geochronological insights into the Proterozoic tectonic evolution of northwestern South America. *Precambrian Research*, *191*(1-2), 58-77. https://doi.org/10.1016/j.precamres.2011.09.005

Ibáñez-Mejía, M., Pullen, A., Arenstein, J., Gehrels, G., Valley, J., Ducea, M., Mora, A., Pecha, M., & Ruiz, J. (2015). Unraveling crustal growth and reworking processes in complex zircons from orogenic lower-crust: The Proterozoic Putumayo Orogen of Amazonia. *Precambrian Research*, *267*, 285-310. https://doi.org/10.1016/j.precamres.2015.06.014

Janoušek, V., Farrow, C. M., & Erban, V. (2006). Interpretation of whole-rock geochemical data in igneous geochemistry:

introducing Geochemical Data Toolkit (GCDkit). *Journal of Petrology, 47*(6), 1255-1259. https://doi.org/10.1093/petrology/egl013

Jaramillo, L. E., & Escovar, R. (1980). *Cinturones de pórfidos cupríferos en las cordilleras colombianas.* Simposio sobre metalogénesis en Latinoamérica, México D.F.

Jiménez-Mejía, D. M. (2003). *Metamorphic and Geochronological Characterization of the Proterozoic Rocks of the Garzón Massif - Southeast of the Colombian Andes* [Master thesis]. Universidade de Sao Paulo.

Jiménez Mejía, D. M., Juliani, C., & Cordani, U. G. (2006). P-T-t conditions of high-grade metamorphic rocks of the Garzon Massif, Andean basement, SE Colombia. *Journal of South American Earth Science*, *21*(4), 322-336. https://doi.org/10.1016/j.jsames.2006.07.001

Kroonenberg, S., & Diederix, H. (1982). *Geology of south–central Huila, uppermost Magdalena Valley, Colombia. A preliminary note.* Guide Book 21 Annual Field Trip Colombian Society Petroleum Geologists and Geophysicists.

Kroonenberg, S. B. (1982). A Grenvillian granulite belt in the Colombian Andes and its relation to the Guiana Shield. *Geologie en Mijnbouw*, *61*(4), 325-333.

Kroonenberg, S. B. (2019). The Proterozoic Basement of the Western Guiana Shield and the Northern Andes. In F. Cediel y R. P. Shaw (eds.), *Geology and Tectonics of Northwestern South America. Frontiers in Earth Sciences* (pp. 115-192). Springer. https://doi.org/10.1007/978-3-319-76132-9_3

Leal-Mejía, H. (2011). *Phanerozoic gold metallogeny in the Colombian Andes: A tectono-magmatic approach* [Ph.D. Thesis]. Universitat de Barcelona.

Leal-Mejía, H., Shaw, R., & Malgrejo, J. C. (2019). Spatial-Temporal Migration of Granitoid Magmatism and the Phanerozoic Tectono- Magmatic Evolution of the Colombian Andes. In F. Cediel y R. P. Shaw (eds.), *Geology and Tectonics of Northwestern South America. Frontiers in Earth Sciences* (pp. 253-410). Springer. https://doi.org/10.1007/978-3-319-76132-9_5

López-Isaza, J. A., & Zuluaga, C. A. (2020). Late Triassic to Jurassic magmatism in Colombia: Implications for the evolution of the northern margin of South America. In J. Gómez & A. O. Pinilla-Pachón (eds.), *The Geology of Colombia* (pp. 77-116, Vol. 2). Servicio Geológico Colombiano. https://doi.org/10.32685/pub.esp.36.2019.03

Mantilla Figueroa, L. C., García, C. A., & Valencia, V. (2016). Propuesta de escisión de la denominada 'Formación Silgará' (Macizo de Santander, Colombia), a partir de edades U-Pb en zircones detríticos. *Boletín de Geología*, *38*(1), 33-47. https://doi.org/10.18273/revbol.v38n1-2016002

Maya, M., & González, H. (1995). Unidades litodémicas en la cordillera Central de Colombia. *Boletín Geológico, 35*(2-3), 43-57. https://doi.org/10.32685/0120-1425/bolgeol35.2-3.1995.316

Núñez, A., & Murillo, A. (1982). *Memoria explicativa: Geología y prospección geoquímica de las planchas 244 Ibagué y 263 Ortega* [Report 1879]. Ingeominas.

Ordoñez-Carmona, O., Pimentel, M. M., & De Moraes, R. (2002). Granulitas de Los Mangos: un fragmento Grenviliano en la parte SE de la Sierra Nevada de Santa Marta. *Revista de la Academia Colombiana de Ciencias Exactas, Físicas y Naturales*, (26), 169-179.

Otamendi, J. E., Ducea M., Cristofolini, E. A., Tibaldi A. M., Camilletti, G. C., & Bergantz G. W. (2017). U-Pb ages and Hf isotope compositions of zircons in plutonic rocks from the central Famatinian arc, Argentina. *Journal of South American Earth Sciences, 76*, 412-426. https://doi.org/10.1016/j.jsames.2017.04.005

Paton, C., Woodhead, J. D., Hellstrom, J. C., Hergt, J. M., Greig, A., & Maas, R. (2010). Improved laser ablation U-Pb zircon geochronology through robust downhole fractionation correction. *Geochemistry, Geophysics, Geosystems*, *11*(3), 36. https://doi.org/10.1029/2009GC002618

Pearce, J. A. (2008). Geochemical fingerprinting of oceanic basalts with applications to ophiolite classification and the search for Archean oceanic crust. *Lithos, 100*(1-4), 14-48. https://doi.org/10.1016/j.lithos.2007.06.016

Peña-Urueña, M. L., Muñoz-Rocha, J. A., & Urueña, C. L. (2018). Laboratorio de Geocronología en el Servicio Geológico Colombiano: avances sobre datación U-Pb en circones mediante la técnica LA-ICP-MS. *Boletín Geológico*, (44), 39-56. https://doi.org/10.32685/0120-1425/boletingeo.44.2018.7

Piraquive, A. (2017). *Marco Estructural: deformaciones y exhumación de los Esquistos de Santa Marta, la acreción e historia de deformación de un terreno caribeño al norte de la Sierra Nevada de Santa Marta* [Ph.D. Thesis]. Universidad Nacional de Colombia.

Profeta, L., Ducea, M. N., Chapman, J. B., Paterson, S. R., Gonzales, S. M. H., Kirsch, M., & DeCelles, P. G. (2015). Quantifying crustal thickness over time in magmatic arcs. *Scientific Reports*, *5*. https://doi.org/10.1038/srep17786

Priem, H. N., P. Andriessen, N. A., Boelrijk, H., De Boorder, E. H., Hebeda, E., Huguett, E., Verdumen, A., & Verschure,

R. (1982). Precambrian Amazonas region of southeastern Colombia (western Guiana Shield). *Geologie en Mijnbouw*, *61*(3), 229-242.

Quandt, D., Trumbull R., Altenberger, W., Cardona, A., Romer, R., Bayona, G., Ducea, M., Valencia, V., Vásquez, M., Cortés, E., & Guzmán, G. (2018). The geochemistry and geochronology of Early Jurassic igneous rocks from the Sierra Nevada de Santa Marta, NW Colombia, and tectono-magmatic implications. *Journal of South American Earth Sciences*, *86*, 216-230. https://doi.org/10.1016/j.jsames.2018.06.019

Quiceno, J., Osorio-Ocampo, S., Vallejo, F., Salazar, A., Ossa, C. A., Giraldo, L., & Romero, L. (2016). Petrografía y geoquímica del Stock de Payandé y su posible relación con el magmatismo Jurásico al sur de Colombia. *Boletín de Geología*, *38*(2), 39-53. https://doi.org/10.18273/revbol.v38n2-2016002

Ramírez, D. A., Correa-Martínez, A. M., Zapata-Villada, J. P., & Rodríguez, G. (2020). Tectono-magmatic implications of the Jurassic volcanic and volcanoclastic record of the Santa Marta Massif (Colombia). *Journal of South American Earth Sciences*, *104*. https://doi.org/10.1016/j.jsames.2020.102866

Ramos, V. A. (2008). The basement of the Central Andes: the Arequipa and related terranes. *Annual Review on Earth and Planetary Sciences*, *36*, 289-324.

Renne, P. R., Swisher, C. C., Deino, A. L., Karner, D. B., Owens, T. L., & DePaolo, D. J. (1998). Intercalibration of standards, absolute agesand uncertainties in ^{40}Ar/^{39}Ar dating. *Chemical Geology, 145*(1-2), 117-152. https://doi.org/10.1016/S0009-2541(97)00159-9

Restrepo-Pace, P. (1995). *Late Precambrian to Early Mesozoic Tectonic Evolution of the Colombian Andes based on new geocronological, geochemical and isotopic date* [Ph.D. Thesis]. The University of Arizona.

Restrepo-Pace, P., & Cediel, F. (2019). Proterozoic Basement, Paleozoic Tectonics of NW South America, and Implications for Paleocontinental Reconstruction of the Americas. In F. Cediel y R. P. Shaw (eds.), *Geology and Tectonics of Northwestern South America*, *Frontiers in Earth Sciences* (pp. 97-112). Springer. https://doi.org/10.1007/978-3-319-76132-9_2

Restrepo, J. J., & Toussaint, J. F. (1989). Terrenos alóctonos en los Andes colombianos: Explicación de algunas paradojas geológicas. In *Memorias V Congreso Colombiano de Geología* [Vol. I, pp. 92-107]. Sociedad Colombiana de Geología.

Restrepo, J. J., Ordóñez-Carmona, O., Martens, U., & Correa, A. M. (2009). Terrenos, complejos y provincias en la cordillera Central colombiana. *Ingeniería, Investigación y Desarrollo*, *9*(2), 49-56.

Restrepo, J. J., & Toussaint, J. F. (2020). Tectonostratigraphic terranes in Colombia: An update. First part: Continental terranes. In J. Gómez y D. Mateus-Zabala (eds.), *The Geology of Colombia* (pp. 37-63, Volume 1). Servicio Geológico Colombiano. https://doi.org/10.32685/pub.esp.35.2019.03

Restrepo, J. J., Martens, U., & Giraldo-Ramírez, W. E. (2020). The Anacona Terrane: A small early Paleozoic peri–Gondwanan terrane in the Cauca–Romeral Fault System. In J. Gómez y D. Mateus-Zabala (eds.), *The Geology of Colombia* (pp. 149-165, Volume 1). Servicio Geológico Colombiano. https://doi.org/10.32685/pub.esp.35.2019.08

Restrepo, J. J., Ordoñez-Carmona, O., Armstrong, R., & Pimentel, M. M. (2011). Triassic metamorphism in the northern part of the Tahamí Terrane of the Central cordillera of Colombia. *Journal of South American Earth Sciences*, *32*(4), 497-507. https://doi.org/10.1016/j.jsames.2011.04.009

Rodríguez, G. (1995a). Petrografía y microtexturas del Grupo Garzón y el Granito de Anatexis de El Recreo, macizo de Garzón, cordillera Oriental-Colombia. *Revista Ingeominas*, (5), 17-36.

Rodríguez, G. (1995b). Petrografía del macizo de La Plata, departamento del Huila. *Revista Ingeominas*, (5), 5-16.

Rodríguez, G., Zapata, G., Velásquez, M. E., Cossio, U., & Londoño, A. C. (2003). Geología de las planchas 367 Gigante, 368 San Vicente del Caguán, 389 Timaná, 390 Puerto Rico, 391 Lusitania (parte noroccidental) y 414 El Doncello, escala 1:100 000 [Explanatory memory]. Ingeominas.

Rodríguez, G., Arango, M. I., Zapata, G., & Bermúdez, J. G. (2016). *Catálogo de unidades litoestratigráficas de Colombia, Formación Saldaña. Cordilleras Central y Oriental Tolima, Huila, Cauca y Putumayo*. Servicio Geológico Colombiano.

Rodríguez-García, G., Obando, G., Correa-Martínez, A. M., Zapata, G., Correa, T., Obando, M., Rincón, A., & Zapata, J. P. (2017a). *Redefinición del bloque norte del Batolito de Ibagué con base en nuevos datos de petrografía, litogeoquímica y geocronología U-Pb*. XVI Congreso Colombiano de Geología, Santa Marta, Colombia.

Rodríguez, G., Zapata, G., Correa-Martínez, A. M., y Arango, M. (2017b). *Caracterización del magmatismo triásico-jurásico del macizo de Santander*. Servicio Geológico Colombiano.

Rodríguez, G., Arango, M. I., Zapata, G., & Bermúdez, J. G. (2018). Petrotectonic characteristics, geochemistry, and U-Pb geochronology of Jurassic plutons in the Upper Magdalena Valley-Colombia: implications on the evolution of magmatic arcs in the NW Andes. *Journal of South American Earth Sciences*, *81*, 10-30. https://doi.org/10.1016/j.jsames.2017.10.012

Rodríguez G., Correa Martínez, A. M., Zapata Villada, J. P., & Obando, G. (2019a). Fragments of a Permian arc on the western margin of the Neoproterozoic basement of Colombia. In *The Geology of Colombia* (Volumen 1, pp. 204-245). Servicio Geológico Colombiano.

Rodríguez, G., Zapata Villada, J. P., Obando, G., Correa Martínez, A. M., Ramírez, D., Muñoz, J. A., Rayo, L. del P., & Ureña, C. L. (2019b). *Batolito de Atánquez Sierra Nevada de Santa Marta Cesar*. Servicio Geológico Colombiano.

Rodríguez, G., & Obando, G. (2020). Volcanism of the La Quinta Formation in the Perijá mountain range. *Boletín Geológico*, (46), 51-94. https://doi.org/10.32685/0120-1425/boletingeo.46.2020.535

Rodríguez-García, G., Correa-Martínez, A. M., Zapata-García, G., Arango-Mejía, M. I., Obando-Erazo, G., Zapata-Villada, J. P., & Bermúdez, J. G. (2020a). Diverse Jurassic magmatic Arcs of the Colombian Andes: Constraints from petrography, geochronology and geochemistry. In J. Gómez y A. O. Pinilla-Pachón (eds.), *The Geology of Colombia* (pp. 77-99, Volume 2). Servicio Geológico Colombiano. https://doi.org/10.32685/pub.esp.36.2019.04

Rodríguez-García, G., Zapata, J. P., Correa-Martínez, A. M., Ramírez, D. A., & Obando, G. (2020b). Aportes al conocimiento del plutonismo del arco Mocoa-Santa Marta durante el Jurásico temprano-medio, en la margen noroccidental de los Andes, Colombia. *Boletín de Geología, 42*(3), 15-50. https://doi.org/10.18273/revbol.v42n3-2020001

Rodríguez, G., Correa Martínez, A. M., Zapata, G., & Arango, M. I. (2020c). Monzogranito de La Corcova. In *Catálogo de las unidades litoestratigráficas de Colombia: Macizo de Santander* (Vol. 1). Servicio Geológico Colombiano. https://doi.org/10.32685/9789585279445.4

Rodríguez, G., Zapata, G., Arango, M. I., & Correa Martínez, A. M. (2020d). Monzogranito de Santa Bárbara. In *Catálogo de las unidades litoestratigráficas de Colombia: Macizo de Santander* (Vol. 1). Servicio Geológico Colombiano. https://doi.org/10.32685/9789585279445.3

Rodríguez, G., Zapata, G., Correa Martínez, A. M., & Arango, M. I. (2020e). Tonalita de San Martín. In *Catálogo de las unidades litoestratigráficas de Colombia: Macizo de Santander* (Vol. 1). Servicio Geológico Colombiano. https://doi.org/10.32685/9789585279445.6

Rodríguez, G., Arango, M. I., Correa Martínez, A. M., & Zapata, G. (2020f). Riolita de San Joaquín. In *Catálogo de las unidades litoestratigráficas de Colombia: Macizo de Santander* (Vol. 1). Servicio Geológico Colombiano. https://doi.org/10.32685/9789585279445.8

Rodríguez, G., Zapata Villada J. P., Correa Martínez A. M., Ramírez, D., Obando, G., Muñoz, J. A., Rayo, L. del P., & Ureña, C. L. (2020g). *Batolito de Pueblo Bello Sierra Nevada de Santa Marta Cesar*. Servicio Geológico Colombiano.

Rodríguez, G., Sabrica, C., Zapata, J. P., Ramírez, D., Correa-Martínez, A. M., Obando, G., & Muñoz, J. A. (2022a). *Catálogo de unidades estratigráficas de Colombia, Granito de Ortega, cordillera Central*. Servicio Geológico Colombiano.

Rodríguez, G., Sabrica, C., Zapata, J. P., Ramírez, D., Correa-Martínez, A. M., Obando, G., & Muñoz, J. A. (2022b). *Catálogo de unidades estratigráficas de Colombia, Granito de La Plata - cordillera Central*. Servicio Geológico Colombiano.

Rodríguez, G., Arango, M. I., Zapata, G., & Bermúdez, J. G. (2022c). Cuarzomonzodiorita del Astillero. In *Catálogo de las unidades litoestratigráficas de Colombia: Valle Superior del Magdalena* (Vol. 2). Servicio Geológico Colombiano. https://doi.org/10.32685/9789585313194.5

Rodríguez, G., Arango, M. I., Bermúdez, J. G., & Zapata, G. (2022d). Cuarzomonzonita de Los Naranjos. In *Catálogo de las unidades litoestratigráficas de Colombia: Valle Superior del Magdalena* (Vol. 2). Servicio Geológico Colombiano. https://doi.org/10.32685/9789585313194.6

Rodríguez, G., Zapata, G., Arango, M. I., & Bermúdez, J. G. (2022e). Monzogranito de Algeciras. In *Catálogo de las unidades litoestratigráficas de Colombia: Valle Superior del Magdalena* (Vol. 2). Servicio Geológico Colombiano. https://doi.org/10.32685/9789585313194.10

Rodríguez, G., Arango, M. I., Zapata, G., & Bermúdez, J. G. (2022f). Granito de Garzón. In *Catálogo de las unidades litoestratigráficas de Colombia: Valle Superior del Magdalena* (Vol. 2). Servicio Geológico Colombiano. https://doi.org/10.32685/9789585313194.11

Rodríguez Ruiz, M. A. (2016). *Geochemistry and petrological characterization of the Payandé stock (Central cordillera, Colombia): crystallization conditions, structural input and geodynamic implications* [Bachelor Thesis]. Universidad de los Andes.

Rubatto, D. (2002). Zircon trace element geochemistry: Partitioning with garnet and the link between U-Pb ages and metamorphism. *Chemical Geology*, *184*(1-2), 123-138. https://doi.org/10.1016/S0009-2541(01)00355-2

Silva-Arias, A., Páez-Acuña, L. A., Rincón-Martínez, D., Tamara-Guevara, J. A., Gómez-Gutiérrez, P. D., López-Ramos, E., Restrepo-Acevedo, S. M., Mantilla-Figueroa, L. C., & Valencia, V. (2016). Basement characteristics in the Lower Magdalena Valley and the Sinú and San Jacinto fold belts: Evidence of a Late Cretaceous magmatic arc at the south of the Colombian Caribbean. *Ciencia, Tecnología y Futuro*, *6*(4), 5. https://doi.org/10.29047/01225383.01

Spikings, R., Cochrane, R., Villagomez, D., Van der Lelij, R., Vallejo, C., Winkler, W., & Beate, B. (2015). The geological history of northwestern South America: from Pangaea to the early collision of the Caribbean Large Igneous Province (290-75 Ma). *Gondwana Research, 27*, 95-139. https://doi.org/10.1016 /j.gr.2014.06.004

Stacey, J. S., & Kramers, J. D. (1975). Approximation of Terrestrial Lead Isotope Evolution by a 2-Stage Model. *Earth and Planetary Science Letters, 26*(2), 207-221. https://doi.org/10.1016/0012-821X(75)90088-6

Streckeisen, A. (1976). Classification and nomenclature of plutonic rocks. *Geologische Rundschau*, *63*(2), 773-786. https://doi.org/10.1007/BF01820841

Streckeisen, A. (1978). IUGS Subcommission on the Systematics of Igneous Rocks: Classification and nomenclature of volcanic rocks, lamprophyres, carbonatites and melilitic rocks; recommendation and suggestions. *Neues Jahrbuch für Mineralogie*, *134*, 1-14.

Tassinari, C. C. G. (1981). *Evolução geotectônica da Província rio Negro-Juruena na região amazônica* [Master Thesis]. Instituto de Geociências, Universidade de São Paulo.

Tassinari, C. C. G., & Macambira, M. J. B. (1999). Geochronological provinces of the Amazonian Craton. *Episodes*, *22*(3), 174-182. https://doi.org/10.18814/epiiugs/1999/v22i3/004

Tazzo-Rangel, D., Weber, B., González-Guzmán, R., Valencia, V., Frei, D., Schaaf, P., & Solari, L. (2018). Multiple metamorphic events in the Palaeozoic Mérida Andes basement, Venezuela: insights from U–Pb geochronology and Hf–Nd isotope systematics. *International Geology Review*, *61*(13), 1557-1593. https://doi.org/10.1080/00206814.2018.1522520

Thompson, A. B., & Connolly, J. A. D. (1995). Melting of the Continental-Crust: Some Thermal and Petrological Constraints on Anatexis in Continental Collision Zones and Other Tectonic Settings. *Journal of Geophysical Research*, *100*, 15565-15579. https://doi.org/10.1029/95JB00191

Toussaint, J. F. (1995). *Evolución geológica de Colombia. Triásico–Jurásico*. Universidad Nacional de Colombia.

Tschanz, C. M., Jimeno, A., & Cruz, J. (1969). *Geology of the Sierra Nevada de Santa Marta (Colombia). Preliminary Report*. Ministerio de Minas y Energía, Instituto Nacional de Investigaciones Geológicas y Mineras y US. Geological Survey.

Tschanz C. M., Cruz, J., Mehnert, H. H., & Cebula, G. T. (1974). Geologic Evolution of the Sierra Nevada de Santa Marta Northeastern Colombia. *GSA Bulletin*, *85*(2), 273-284. https://doi.org/10.1130/0016-7606(1974)85<273:GEOTS-N>2.0.CO;2

Van der Lelij, R., Spikings, R., & Mora, A., (2016). Thermochronology and tectonics of the Mérida Andes and the Santander Massif, NW South America. *Lithos*, *248-251*, 220-239. https://doi.org/10.1016/j.lithos.2016.01.006

Van der Lelij, R., Spikings, R., Gerdes, A., Chiaradia, M., Vennemann, T., & Mora, A. (2019). Multi-proxy isotopic tracing of magmatic sources and crustal recycling in the Palaeozoic to Early Jurassic active margin of North-Western Gondwana. *Gondwana Research*, *66*, 227-245. https://doi.org/10.1016/j.gr.2018.09.007

Velandia, F., Ferreira, P., Rodríguez, G., & Núñez, A. (1996). Memoria explicativa levantamiento geológico de la Plancha 366 - Garzón. Ingeominas.

Velandia, F., Núñez, A., & Marquínez, G. (2001). Mapa geológico departamento del Huila. Escala 1:300 000 [Explanatory memory). Ingeominas.

Villagómez, D., Spikings, R., Magna, T., Kammer, A., Winkler, W., & Beltrán, A. (2011). Geochronology, geochemistry and tectonic evolution of the Western and Central cordilleras of Colombia. *Lithos*, *125*, 875-896. https://doi.org/10.1016/j.lithos.2011.05.003

Villagómez, D., Martens U., & Pindell J. (2015). *Are Jurassic and some older blocks in the northern Andes in-situ or far-travelled? Potential correlations and new geochronological data from Colombia and Ecuador*. Symposium: Tectónica Jurásica en la parte noroccidental de Sur América y bloques adyacentes.

Villamizar-Escalante, N., Bernet, M., Urueña-Suárez, C., Hernández-González, J. S., Terraza-Melo, R., Roncancio, J., Muñoz, J. A., Peña, M. L., Amaya, S., & Piraquive, A. (2021). Thermal history of the southern Central Cordille-

ra and its exhumation record in the Cenozoic deposits of the Upper Magdalena Valley, Colombia. *Journal of South American Earth Sciences, 107*. https://doi.org/10.1016/j.jsames.2020.103105

Ward, D. E., Goldsmith, R., Cruz B., J., & Restrepo A., H. (1973). Geología de los cuadrángulos H-12 Bucaramanga y H-13 Pamplona, departamento de Santander. *Boletín Geológico, 21*(1-3), 1-134. https://doi.org/10.32685/0120-1425/bolgeol21.1-3.1973.383

Wiedenbeck, M., Allé, P., Corfu, F., Griffin, W. L., Meier, M., Oberli, F., von Quadt, A., Roddick, J. C., & Spiegel, W. (1995). Three natural zircon standards for U-Th-Pb, Lu-Hf, trace element and REE analyses. *Geostandards Newsletter, 19*(1), 1-23. https://doi.org/10.1111/j.1751-908X.1995.tb00147.x

Zapata, S., Cardona, A., Jaramillo, C., Valencia, V., & Vervoort, J. (2016). U-Pb LA-ICP-MS geochronology and geochemistry of Jurassic volcanic and plutonic rocks from the Putumayo region (southern Colombia): tectonic setting and regional correlations. *Boletín de Geología, 38*(2). https://doi.org/10.18273/revbol.v38n2-2016001

Zapata, G., Rodríguez, G., & Arango, M. I. (2017). Petrografía, geoquímica y geocronología de rocas metamórficas aflorantes en San Francisco Putumayo y la vía Palermo-San Luis asociadas a los complejos La Cocha–Río Téllez y Aleluya. *Boletín de Ciencias de la Tierra, 41*, 47-64.

Zapata, G., Correa Martínez, A. M., Rodríguez, G., & Arango, M. I. (2020a). Granito de Pescadero. In *Catálogo de las unidades litoestratigráficas de Colombia: Macizo de Santander* (Vol. 1). Servicio Geológico Colombiano. https://doi.org/10.32685/9789585279445.2

Zapata, G., Arango, M. I., Correa Martínez, A. M., & Rodríguez, G. (2020b). Riolitas El Uvo. In *Catálogo de las unidades litoestratigráficas de Colombia: Macizo de Santander* (Vol. 1). Servicio Geológico Colombiano. https://doi.org/10.32685/9789585279445.7

Zapata, G., Rodríguez, G., Arango, M. I., & Bermúdez, J. G. (2022). Cuarzomonzodiorita de Páez. In *Catálogo de las unidades litoestratigráficas de Colombia: Valle Superior del Magdalena* (Vol. 2). Servicio Geológico Colombiano. https://doi.org/10.32685/9789585313194.3

Zapata-Villada, J. P., Rodríguez, G., Correa-Martínez, A. M., Ramírez, D., & Obando, G. (2020). *Catálogo de unidades estratigráficas de Colombia, Batolito de Patillal*. Servicio Geológico Colombiano.

Zapata-Villada, J. P., Rodríguez, G., Ramírez, D., Correa-Martínez, A. M., Obando, G., & Muñoz, J. A. (2022). *Catálogo de unidades litoestratigráficas de Colombia, Complejo Icarcó*. Servicio Geológico Colombiano.

Zuluaga, C., Pinilla, A., & Mann, P. (2015). Jurassic silicic volcanism and associated continental- arc basin in Northwestern Colombia (southern boundary of the Caribbean plate). In C. Bartolini y P. Mann (eds.), *Petroleum geology and potential of the Colombian Caribbean margin, AAPG memoir* (pp 137-160). American Association of Petroleum Geologists.

Zuluaga, C. A., Amaya, S., Urueña, C., & Bernet, M. (2017). Migmatization and low-pressure overprinting metamorphism as record of two pre-Cretaceous tectonic episodes in the Santander Massif of the Andean basement in northern Colombia (NW South America). *Lithos, 274-275*, 123-146. https://doi.org/10.1016/j.lithos.2016.12.036

Zuluaga, C., & López, J. (2019). Ordovician Orogeny and Jurassic Low-Lying Orogen in the Santander Massif, Northern Andes (Colombia). In F. Cediel y R. P. Shaw (eds.), *Geology and Tectonics of Northwestern South America, Frontiers in Earth Sciences* (pp. 195-250). Springer. https://doi.org/10.1007/978-3-319-76132-9_4